UNIVERSIDADE ESTADUAL DE MARINGÁ
CENTRO DE CIÊNCIAS BIOLÓGICAS
PROGRAMA DE PÓS-GRADUAÇÃO EM CIÊNCIAS BIOLÓGICAS

MARIANA MARQUES NOGUEIRA WENDT

VIA DAS PENTOSES FOSFATO E OXIDAÇÃO DE ÁCIDOS GRAXOS NO FIGADO DE RATOS COM ARTRITE INDUZIDA POR ADJUVANTE

Maringá
2018

MARIANA MARQUES NOGUEIRA WENDT

VIA DAS PENTOSES FOSFATO E OXIDAÇÃO DE ÁCIDOS GRAXOS NO FIGADO DE RATOS COM ARTRITE INDUZIDA POR ADJUVANTE

Tese apresentada à Universidade Estadual de Maringá, como requisito parcial para a obtenção do título de doutor.

Orientador: Dr. Jurandir Fernando Comar

Maringá
2018

MARIANA MARQUES NOGUEIRA WENDT

VIA DAS PENTOSES FOSFATO E OXIDAÇÃO DE ÁCIDOS GRAXOS NO FIGADO DE RATOS COM ARTRITE INDUZIDA POR ADJUVANTE

Tese apresentada à Universidade Estadual de Maringá, como requisito parcial para a obtenção do título de doutor.

Aprovado em: 26/02/2018

BANCA EXAMINADORA

_____

Prof. Dr Jurandir Fernando Comar
Universidade Estadual de Maringá

_____

Prof. Dra Alessandra Lourenço Cecchini Armani
Universidade Estadual de Londrina

_____

Prof. Dra Maria Ida Bonini Ravanelli Speziali
Universidade Estadual de Maringá

_____

Prof. Dr Sidney Barnabé Peres
Universidade Estadual de Maringá

_____

Prof. Dra Maria Montserrat Diaz Pedrosa
Universidade Estadual de Maringá

BIOGRAFIA

Mariana Marques Nogueira nasceu em Rolim de Moura/RO em 27/02/1988. Possui graduação em Ciências Biológicas- Licenciatura e Bacharelado (2010) pela Universidade Estadual do Norte do Paraná – *campus* Luiz Meneghel e Mestrado em Biologia Celular e Molecular (2013) pela Universidade Estadual de Maringá. Desenvolveu o trabalho de mestrado e doutorado sob a orientação do professor Dr. Jurandir Fernando Comar, no Laboratório de Metabolismo Hepático, Departamento de Bioquímica.

Dedico este trabalho a minha filha Catarina

AGRADECIMENTOS

Agradeço ao meu orientador, por toda a orientação, confiança e amizade. A professora Anacharis pelos ensinamentos e pela amizade desde o inicio da minha caminhada, no mestrado.

Aos meus amigos feitos nessa jornada, Gabriela, Ângela, Amanda, Cristiane, Geferson e Ana Paula, quero agradecer não só pela ajuda, mas pela amizade, ensinamentos, risadas e pelo apoio nos momentos mais dificies. Aos outros alunos do nosso laboratório Juliana, Lucas, Lorena, Heloisa, Luciana e Mellina, pela compreensão. E quero agradecer a todos eles pelos momentos de descontração.

Quero agradecer principalmente ao meu marido e minha filha, que tornaram os meus dias mais felizes. Toda a compreensão, companheirismo, paciência e incentivo foram fundamentais nessa caminhada. Aos meus pais, que sempre incentivaram meus estudos e sempre me apoiaram. A minha irmã, que sempre me ajudou nos momentos em que eu precisava de concentração, brincando e passeando com a sobrinha.

E ao apoio financeiro do CNPq e da CAPES.

“Todas as vitórias ocultam uma abdicação.”

(Simone de Beauvoir)

APRESENTAÇÃO

Este é um trabalho realizado no Laboratório de Metabolismo Hepático e Radioisótopos do Departamento de Bioquímica e no Laboratório de Inflamação do Departamento de Farmacologia e Terapêutica da Universidade Estadual de Maringá, apresentado na forma de dois artigos científicos originais, em consonância com as regras do Programa de Pós-graduação em Ciências Biológicas.

Artigo 1:

Mariana M. N. Wendt, Gabriela B. Franco-Salia, Lorena C. Santos, Ângela V. Parizotto, Ciomar A. Bersani-Amado, Adelar Bracht, Jurandir F. Comar. **Fatty acids uptake and oxidation are increased in the liver of rats with adjuvant-induced arthritis**. Journal of Cellular Biochemistry, submetido.

Artigo 2:

Mariana M. N. Wendt, Ângela V. Parizotto, Ciomar A. Bersani-Amado, Adelar Bracht, Jurandir F. Comar. **Pentose monophosphate pathway is stimulated in the liver of arthritic rats.** Biochimie, a ser submetido.

LIST OF ABBREVIATIONS AND ACRONYMS

ACC	acetyl-CoA carboxylase
CAT I	carnitine acyltransferase I
CAT II	carnitine acyltransferase II
CEEA	Ethics Committee for Animal Experimentation
CoA	coenzyme A
CS	citrate synthase
FA	fatty acids
FFA	free fatty acids
FAS	fatty acid synthase
FAT/CD36	fatty acids translocase/CD36
GSH	reduced glutathione
GSSG	oxidized glutathione
G6PDH	glucose 6-phosphate dehydrogenase
HDL	high density lipoprotein
HPLC	high-performance liquid chromatography
IL-1	interleukin 1
IL-6	interleukin 6
LDL	low density lipoprotein
LBM	loss of body mass.
MCT1	monocarboxylate transporter 1
MDH	malate dehydrogenase
NFkB	nuclear factor kappa B
Nfr2	nuclear factor erythroid 2-related 2
PGC-1α	peroxisome proliferator-activated receptor gama
PPAR-γ	coactivator-1 alpha
PPP	pentose phosphate pathway
ROS	reactive oxygen species
TAL	transaldolase
TG	triglycerides
TNF-α	tumoral necrosis factor alpha
VLDL	very low density lipoprotein

RESUMO GERAL

INTRODUÇÃO: A artrite reumatoide é uma doença inflamatória crônica e sistêmica de natureza autoimune que causa a destruição progressiva das articulações e está associada à mortalidade prematura. Além da inflamação, o estresse oxidativo está aumentado tanto nas articulações como sistemicamente. Alterações metabólicas são proeminentes na artrite reumatoide, como a perda da massa muscular, conhecida como caquexia reumatoide. Aproximadamente 10% dos pacientes artriticos desenvolvem um estagio da caquexia associada às doenças cônicas, em que o perda muscular está associado a perda de massa adiposa e redução do peso corporal. Esta ultima condição é conhecida como caquexia reumatoide grave, a qual está associada à dislipidemia e uma maior predisposição a doenças cardiovasculares. Os niveis circulantes de triglicerídeos (TG) e acidos graxos livres (FFA) ainda não foram definidos de forma consistente na artrite severa. Da mesma forma, o metabolismo de lipidios é desconhecido no fígado artrítico. Para preencher esta lacuna, o presente estudo caracterizou perfil lipídico plasmático e a captação e metabolismo de ácidos graxos livres no fígado perfundido de ratos com artrite induzida por adjuvante, uma imunopatologia experimental em ratos que compartilha diversas carcteristicas com a artrite reumatoide severa. Além da caquexia e da resposta inflamatória generalizada, o estresse oxidativo está igualmente aumentado sistemicamente em ratos artríticos. Particularmente no fígado, onde as alterações metabólicas são proeminentes, o estresse oxidativo é mais pronunciado quando comparado à outros órgãos. A estimulação do sistema pró-oxidante, induzida por citocinas, contribui para um aumento do estresse oxidativo hepático na artrite, entretanto, uma redução acentuada da razão GSH/GSSG aparenta ser crítica para modificar o estado oxidativo do órgão. Esse último, por sua vez, é atribuido a um ambiente celular mais oxidado, particularmente uma redução da razão NADPH/$NADP^+$, que pode ser o resultado de uma deficiência na atividade da via das pentoses fosfato citosólica. Portanto, este estudo também teve como objetivo determinar o conteúdo hepático de nucleotídeos de adenina e o fluxo de glicose através da via das pentoses fosfato (PPP) no fígado de ratos artritcos, que por sua vez, deveria permitir extrapolações para pacientes como artrite rematoide severa. **MÉTODOS**: A indução da artrite foi realizada em ratos machos da linhagem Holtzman (180-200g) com o adjuvante

completo de Freund. Ratos com idade e peso similares foram utilizados como controle. TG, FFA, glicerol, colesterol total, colesterol HDL e corpos cetônicos foram dosados no plasma utilizando métodos enzimáticos. TG, colestetol total, glicogênio e glicose 6-fosfato foram adicionalmente determinados no fígado. Os niveis hepáticos de NADH, NADPH, NAD^+, $NADP^+$, ATP, ADP, AMP, GSH e GSSG foram determinados utilizando HPLC. A atividade do ciclo do ácido citrico foi avaliada em fígados perfundidos com [1-^{14}C]ácido octanoico. A produção hepática de CO_2 e corpos cetônicos, provenientes do catabolismo de de ácidos graxos foi avaliada em fígados perfundidos utilizando ácidos [1-^{14}C]ácido palmítico e [1-^{14}C]ácido oleico. A atividade da PPP foi avaliada em fígados perfundidos com [1-^{14}C]glicose e [6-^{14}C]glicose. A atividade de carnitina acil transferase I e II (CAT I e II), acetil CoA carboxilase (ACC), glucose-6-fosfato desidrogenase (G6PDH) e transaldolase (TAL) foram adicionalmente avaliadas no fígado. **RESULTADOS:** Após 18 dias da indução da artrite, os animais desenvolveram uma caquexia severa. Os resultados obtidos para ratos artriticos podem ser resumidos da seguinte forma: (1) os níveis de TG e colesterol toal forma diminuidos no plasma (10-20%) e no fígado (20-35%); (2) os níveis de FFA e glicerol foram aumentados, enquanto que os níveis de corpos cetônicos foram diminuidos no plasma; (3) a captação e oxidação dos ácidos palmitico e oleico foram aumentadas no fígado; (4) a cetôgenese não diferiu, mas os corpos cetônicos circulantes diminuiram (45%); (5) a razão hepática de β-hidroxibutirato/acetoacetato, um indicador da razão mitocondrial de NADH/NAD^+, foi reduzida (85%); (6) a atividade do ciclo do ácido citrico no fígado foi aumentado no jejum e no estado alimentado; (7) as razões NADH/NAD^+ e NADPH/$NADP^+$ foram reduzidas em aproximadamente 30% no fígado dos animais em jejum e alimentados; (8) a atividade da CAT I não diferiu, mas a atividade da CAT II e ACC foram diminuidas no fígado; (9) os níveis hepáticos de GSH e a razão GSH/GSSG diminuiram; (10) o conteúdo hepático da glutationa total (GSH+ 2xGSSG) e dinucleotideos fosfato (NADPH + $NADP^+$) foram fortemente reduzidos; (11) os níveis hepáticos de glicogênio foram aproximadamente um quarto dos niveis controles; (12) os níveis hepáticos de glicose 6-fosfato foram aumentados (20-30%) nos animais alimentados e em jejum; (13) o fluxo de glicose através da PPP foi aumentada em 60%; e (14) a atividade da G6PDH e TAL foram aumentadas no fígado, mas apenas no estado de jejum. **DISCUSSÃO E CONCLUSÃO**: Os resultados do presente estudo

revelaram que o aumento de acidos graxos livres e glicerol circulantes parece ser consequência de uma lipólise acentuada no tecido adiposo, induzido por citocinas, associado a uma reduzida absorção periférica pelo tecido muscular esquelético e cardiaco. A maior absorção de ácidos graxos livres no fígado reflete a sua maior oxidação no órgão. Por sua vez, a maior oxidação de ácidos palmitico e oléico aparenta ser consequência de um ambiente mais oxidado nas células hepáticas de ratos artriticos. Além disso, os baixos niveis de TG circulantes e hepáticos parecem ser causados pelo aumento da oxidação associada à síntese reduzida de acidos graxos no fígado de ratos artriticos. Esses resultados revelam que, ao contrário de outras doenças inflamatórias crônicas, o metabolismo lipidico hepático em ratos artríticos ocorre em direção ao estado catabólico, uma condição que certamente contibui para a caquexia severa verificada em ratos com artrite induzida por adjuvante e, possivelmente, na artrite reumatoide grave. Além disso, os níveis elevados de FFA circulantes são considerados pró-aterogênicos e se associados com uma elevada inflamação podem contribuir para uma maior ocorrência da doença cardiovascular na artrite reumatoide severa. O motivo pela qual os pares NADPH-$NADP^+$ e NADH-NAD^+ são deslocados em direção ao estado mais oxidado no fígado artrítico pode ser atribuído a um estresse oxidativo pronunciado associado a um metabolismo oxidativo acelerado no órgão. O estresse oxidativo é consequencia de um sistema antioxidante prejudicado, particularmente à uma diminuída razão GSH/GSSG, associada a uma produção aumentada de ROS. O estresse oxidativo pronunciado consome uma quantidade excessiva de equivalentes redutores para neutralizar sem sucesso a intensa produção de ROS e, portanto, diminuir a razão NADPH/$NADP^+$ no figado artrítico. Este último associado a um aumento dos níveis de glicose 6-fosfato estimula o fluxo de glicose através de PPP em ratos artríticos e, por extensão, a regeneração de NADPH. Como a atividade da glutationa redutase não é modificada e um dos substratos desta enzima, o GSSG, não diminui no fígado artrítico, o outro substrato, NADPH, está possivelmente limitando a regeneração de GSH no fígado artrítico. Assim, esses resultados revelam adicionalmente que o estresse oxidativo acentuado no fígado de ratos artríticos excede a regeneração de NADPH na PPP e esse fenômeno é possivelmente a consequência do conteúdo hepático reduzido de adenina nucleotídeos fosfato (NADPH + $NADP^+$) e glutationa (GSH + 2GSSG).

Palavras chave: Artrite induzida por adjuvante; caquexia reumatoide; catabolismo de ácidos graxos; via das pentoses fosfato.

GENERAL ABSTRACT

BACKGROUND: Rheumatoid arthritis is a systemic autoimmune and chronic inflammatory disease that leads to progressive joint destruction and it is associated with premature mortality. In addition to inflammation, oxidative stress is increased in joints and systemically. Metabolic alterations are also prominent in rheumatoid arthritis, such as the muscle wasting condition known as rheumatoid cachexia. Nearly 10% of arthritic patients experience the stage of chronic wasting diseases, in which muscle wasting is associated with adipose tissue wasting and reduced body weight. The latter is the severe rheumatoid cachexia, which is associated with dyslipidemia and higher predisposition to cardiovascular diseases. Circulating levels of triglycerides (TG) and free fatty acids (FFA) have not yet been consistently defined in severe arthritis. Similarly, the metabolism of these lipids in the arthritic liver has not yet been clarified. Aiming at filling these gaps the present study presents a characterization of the circulating lipid profile and of the fatty acids uptake and metabolism in perfused livers of rats with adjuvant-induced arthritis, an experimental immunopathology in rats which shares many features with severe rheumatoid arthritis. In addition to cachexia and generalized inflammatory response, oxidative stress is altered systemically in these animals. Particularly in the liver, where metabolic modifications have been reported, oxidative stress is quite pronounced when compared to other organs. The cytokine-induced stimulation of the pro-oxidant system contributes significantly to the oxidative stress in the arthritic liver. However, the ratio of reduced to oxidized glutathione (GSH/GSSG) is decreased in the liver of arthritic rats and it seems to be critical to modify this condition. The ratio of NADPH to $NADP^+$ has been suggested to be decreased and intensifying the oxidative stress in the organ. The cytosolic pentose phosphate pathway (PPP) is the major via to regenerate NADPH from $NADP^+$ in the liver cells and, therefore, the present study also aimed to measure the hepatic content of adenine nucleotides and to estimate the flux of glucose through the PPP in the liver of arthritic rats. The latter should allow extrapolations for patients with rheumatoid arthritis. **METHODS**: Induction of arthritis was performed in *Holtzman*

rats (180-200 g) with Freund's adjuvant and animals with similar ages were controls. TG, FFA, glycerol, total and HDL cholesterol and ketone bodies were assayed in the plasma by enzymatic methods. TG, total cholesterol, glycogen and glucose 6-phosphate were additionally measured in the livers. The hepatic levels of NADH, NADPH, NAD^+, $NADP^+$, ATP, ADP, AMP, GSH and GSSG were determined using HPLC. Metabolic pathways was evaluated in the perfused livers with [1-^{14}C]octanoic acid (citric acid cycle), [1-^{14}C]palmitic and [1-^{14}C]oleic acids (fatty acids catabolism and ketogenesis) and with [1-^{14}C]glucose and [6-^{14}C]glucose (activity of PPP). The activity of carnitine acyl transferase I and II (CAT I and II), acetyl CoA carboxylase (ACC), glucose 6-phosphate dehydrogenase (G6PDH) and transaldolase were additionally assessed in the livers. **RESULTS**: At 18 days after adjuvant injection, arthritic rats developed a generalized inflammatory and severe cachexia. The results obtained in the present study show that in arthritic rats, (1) the levels of TG and total cholesterol were decreased in the plasma (10-20%) and liver (20-35%); (2) the levels of FFA and glycerol were increased whereas ketone bodies were decreased in the plasma; (3) the uptake and oxidation of palmitic and oleic acids were increased in the liver; (4) ketogenesis was not different, but circulating ketone bodies were reduced (45%); (5) the hepatic ratio of β-hydroxybutyrate to acetoacetate, an indicator of mitochondrial NADH/NAD^+ ratio, was strongly reduced (85%); (6) the hepatic citric acid cycle activity was increased in the fed state; (7) the ratio of NADH to NAD^+ and NADPH to $NADP^+$ were reduced by approximately 30% in the livers of both fasted and fed animals; (8) the activity of CAT I was not different, but the activity of CAT II and ACC were decreased in the liver; (9) hepatic levels of GSH and the ratio of GSH to GSSH ratio were diminished; (10) hepatic content of total glutathione (GSH + 2xGSSG) and dinucleotides phosphate (NADPH + $NADP^+$) were strong reduced; (11) hepatic levels of glycogen was only one quarter of that in control rats; (12) hepatic levels of glucose 6-phosphate were increased (20-30%) in the fed and fasted conditions; (13) the flux of glucose through PPP was increased by 60% in the liver; and (14) the activity of G6PDH and transaldolase were increased in the livers, but only in the fasted state. **DISCUSSION AND CONCLUSION**: The increased levels of circulating FFA and glycerol in arthritic rats are possibly the consequence of a cytokine-induced adipose tissue lipolysis associated with reduced peripheral uptake, particularly in skeletal muscle and heart muscle. The higher uptake of FFA in the

livers of arthritic rats reflects their higher oxidation in the organ. In turn, the higher oxidation of both palmitic and oleic acids is possibly the consequence of a more oxidized state of the arthritic livers due to a pronounced oxidative stress and accelerated mitochondrial respiration. In addition, the lower levels of circulating and hepatic TG seem to be caused by an increased oxidation associated to a reduced synthesis of fatty acids in arthritic livers. These results reveal that, as opposed to other chronic wasting diseases, the hepatic metabolism in arthritic rats occurs toward to catabolic state, a condition that should certainly contribute to the marked cachexia verified in rats with adjuvant-induced arthritis and possibly in the severe rheumatoid arthritis. In addition, high levels of circulating FFA are considered itself proatherogenic and further associated with high grade of inflammation can be contributing to greater occurrence of cardiovascular disease in the severe rheumatoid arthritis. The reason by which the NADH-NAD^+ and NADPH-$NADP^+$ couples are shifted toward an oxidized state in the arthritic liver has not yet been completely clarified, but it has been attributed to the pronounced oxidative stress associated to the accelerated oxidative metabolism in the organ. The altered oxidative stress is consequence of an impaired antioxidant system, particularly a reduced ratio of GSH to GSSG, associated to an increased cytokine-mediated production of ROS. The pronounced oxidative stress consumes excessive amount of reducing equivalents to unsuccessfully neutralize the more intense ROS production and, therefore, decrease the NADPH/$NADP^+$ ratio in the arthritic liver. The latter associated with an increased levels of glucose 6-phosphate stimulate the flux of glucose through PPP in arthritic rats and, by extension, the NADPH regeneration. As the activity of glutathione reductase is not modified and one of the substrates of this enzyme, GSSG, is not decreased in the arthritic liver, the other substrate, NADPH, is possibly limiting the GSH regeneration in the arthritic liver. Thus, these results reveal in addition that the accentuated oxidative stress in the liver of arthritic rats exceeds the rate of NADPH regeneration in the PPP and this phenomenon is possibly the consequence of the reduced hepatic content of total adenine dinucleotides phosphate (NADPH + $NADP^+$) and glutathione (GSH + 2GSSG).

Key Words: adjuvant-induced arthritis; rheumatoid cachexia; fatty acids catabolism; pentose phosphate pathway

Fatty acids uptake and oxidation are increased in the liver of rats with adjuvant-induced arthritis

Mariana M. N. Wendt[1], Gabriela B. Franco-Salla[1], Lorena S. Castro[1], Ângela V. Parizotto[1], Ciomar A. Bersani-Amado[2], Adelar Bracht[1], Jurandir F. Comar[1*]

[1] Department of Biochemistry, State University of Maringa, PR, Brazil

[2] Department of Pharmacology and Therapeutics, State University of Maringa, PR, Brazil

Address for correspondence:
*Jurandir Fernando Comar
Department of Biochemistry
University of Maringá
87020900 Maringá, Brazil
Email: jurandircomar@yahoo.com.br

Running head: Fatty acids oxidation in the arthritic liver

Total number of text figures and tables: 11

Grant sponsor: Conselho Nacional de Desenvolvimento Científico e Tecnológico (CNPq); Grant number: 447876/2014-7

ABSTRACT

Severe rheumatoid cachexia is associated with pronounced loss of muscle and fat mass in patients with advanced rheumatoid arthritis. This condition affects nearly 10% of all patients and it is associated with dyslipidemia and predisposition to cardiovascular diseases. Circulating levels of triglycerides and free fatty acids have not yet been consistently defined in severe arthritis. Similarly, the metabolism of these lipids in the arthritic liver has not yet been clarified. Aiming at filling these gaps the present study presents a characterization of the circulating lipid profile and of the fatty acids uptake and metabolism in perfused livers of Holtzman rats with adjuvant-induced arthritis. The contents of hepatic adenine nucleotides were additionally assessed to evaluate the cellular redox status. The levels of triglycerides (TG) and total cholesterol were reduced in both serum (10-20%) and liver (20-35%) of arthritic rats. The levels of circulating free fatty acids (FFA) were 40% higher in arthritic rats, possibly in consequence of cytokine-induced adipose tissue lipolysis. Hepatic uptake and oxidation of both palmitic and oleic acids was higher in arthritic livers. The phenomenon is possibly the consequence of a more oxidized state of the arthritic livers due to a pronounced oxidative stress and accelerated mitochondrial respiration. Ketogenesis was not different in arthritic rats, but the circulating ketone bodies were 45% lower. The β-hydroxybutyrate/acetoacetate ratio, an indicator of the mitochondrial NADH/NAD^+ ratio, was 85% lower in arthritic livers, which presented higher activities of the citric acid cycle driven by both endogenous and exogenous fatty acids. The ratios of NADPH/$NADP^+$ and NADH/NAD^+ were approximately 30% lower in arthritic livers. The lower levels of circulating and hepatic TG seem to be caused by an increased oxidation associated to a reduced synthesis of fatty acids in arthritic livers. These results reveal that the lipid hepatic metabolism in arthritic rats presents a strong catabolic tendency, a condition that should contribute to the marked cachexia described for arthritic rats and possibly for the severe rheumatoid arthritis.

Key words*: adjuvant-induced arthritis, rheumatoid cachexia, liver metabolism, perfused rat liver, fatty acids catabolism.*

Abbreviations: FFA, free fatty acids; FA, fatty acids; TG, triglycerides; HDL, high density lipoprotein; LDL, low density lipoprotein; VLDL, very low density lipoprotein; ROS, reactive oxygen species; GSH, reduced glutathione; GSSG, oxidized glutathione; TNF-α, tumoral necrosis factor alpha; IL-1 and 6, interleukin 1 and 6; NFkB, nuclear factor kappa B; FAS, fatty acid synthase; ACC, acetyl-CoA carboxylase; MDH, malate dehydrogenase; CS, citrate synthase; CAT I and II, carnitine acyltransferase I and II; CoA, coenzyme A; (FAT)/CD36, fatty acids translocase/CD36; MCT1, monocarboxylate transporter 1; PGC-1α, peroxisome proliferator-activated receptor gama (PPAR-γ) coactivator-1 alpha; HPLC, high-performance liquid chromatography; LBM, loss of body mass.

INTRODUCTION

Rheumatoid arthritis is an autoimmune and chronic inflammatory disease that leads to progressive joint destruction. The pathophysiology of arthritis involves an intense hyperplasia of the synovial membrane and cartilage with participation of proinflammatory cytokines and overproduction of reactive species [Misko et al., 2013]. Rheumatoid arthritis is a systemic disease and in addition to the joints it affects other organs, such as brain, liver and muscles [Mcinnes & Schett, 2011]. It affects nearly 1.0% of the adult population worldwide and is associated with progressive disability and premature mortality, mainly due to cardiovascular complications [Kitas & Gabriel, 2011].

Metabolic alterations are prominent in rheumatoid arthritis, particularly the muscle wasting condition known as rheumatoid cachexia, which occurs in approximately two-thirds of all patients and is related to dyslipidemia, metabolic syndrome and cardiovascular disease [Kitas & Gabriel, 2011; Roubenoff, 2009]. In rheumatoid cachexia, muscle wasting normally occurs with unaltered body weight, however, nearly 10% of the patients experience a stage of chronic wasting disease, in which muscle wasting is associated with adipose wasting and reduced body weight [von Haehling & Anker, 2014; Summers et al., 2010]. The latter occurs in severe and uncontrolled rheumatoid arthritis and is associated with an even greater occurrence of cardiovascular disease and mortality [Summers et al., 2010]. Arthritic cachexia is mediated by cytokines, particularly tumor necrosis factor-alpha (TNF-α), interleukin 1 (IL-1) and IL-6, which stimulate the whole-body protein breakdown and additionally adipose lipolysis [Mazuko, 2014].

Increased risk for cardiovascular diseases in rheumatoid arthritis is also associated with altered lipid metabolism, however, this relationship has been not yet fully clarified [Zegkos et al., 2016; Mazuko, 2014]. Hyperlipidemia is not common, but dyslipidemia is frequent and affects approximately 60% of patients, which present reduced levels of plasma HDL cholesterol, normal or even diminished total cholesterol and, consequently, diminished total /HDL cholesterol ratio [Zegkos et al., 2016; Choy et al., 2014; Robertson et al., 2013]. The plasma levels of total cholesterol are further reduced in severe arthritis and they are related to an even higher incidence of cardiovascular diseases [Zegkos et al., 2016; Myasoedova et al., 2011]. The plasma

cholesterol profile in severe rheumatoid arthritis is similar to that found in other chronic wasting diseases. However, the reports about the levels of triglycerides (TG) and free fatty acids (FFA; non esterified fatty acids) present inconsistencies as reductions, no alterations and even increases have been variously reported [Choy & Sattar, 2009; Sattar et al., 2003; Munro et al., 1997].

The body fat storage and plasma levels of lipids result from an integrated metabolism of adipose tissue, muscle and liver [Frayn et al., 2006]. High levels of plasma FFA occur as the result of increased adipose lipolysis associated with reduced FFA uptake in muscle and liver [Frayn et al., 2006]. Hypertriglyceridemia occurs as the result of increased hepatic synthesis of fatty acids (FA) and TG associated with reduced peripheral uptake [Gonzalez-Gay et al., 2005]. It has been proposed that in rheumatoid arthritis proinflammatory cytokines stimulate adipose lipolysis, hepatic synthesis of FA and TG and inhibit peripheral lipoprotein lipase, what together culminates in high plasma levels of TG, and perhaps FFA [Gonzales-Gay et al., 2005; Sattar et al., 2003]. However, it has been also claimed that severe inflammation promotes consumption and reduces the synthesis of lipoproteins, resulting in lower levels of TG in advanced and uncontrolled rheumatoid arthritis [Zegkos et al., 2016; Kitas & Gabriel, 2011]. These assumptions seem contradictory and in fact they lack experimental confirmation as they were extrapolated from a set of data relating cachexia to accelerated atherogenesis in chronic wasting diseases [Delano & Moldawer, 2006; Khovidhunkit et al., 2000]. It is known that lipolysis is increased in severe arthritis, however, high levels of plasma FFA do only occur if their uptake is reduced, especially in the liver, which plays a central role in the body lipid homeostasis [Summers et al., 2010].

The hepatic lipid metabolism has been proposed to be similarly modified for most chronic wasting diseases and can be summarized as follows: increased FFA uptake and synthesis associated to increased TG synthesis and release [Delano & Moldawer, 2006]. However, there is no evidence that this status applies to rheumatoid arthritis, particularly during periods of high activity of the disease. Modifications of the intermediary metabolism are generally peculiar to each illness. Serious hepatic complications are rare in rheumatoid arthritis, however, the liver helps to worsen the inflammation by secreting acute phase proteins and reducing albumin synthesis [Mcinnes & Schett, 2011]. Metabolic

modifications have also been found in perfused livers of rats with arthritis induced by adjuvant. They consist in accelerated oxidative metabolism, reduced gluconeogenesis and increased glycolysis [Castro-Ghizoni et al., 2017; Fedatto et al., 2000]. This indicates that, at least for glucose, hepatic metabolism in arthritis seems to be characterized by a prevalence of catabolic over anabolic pathways, in disagreement to what has been reported for other chronic wasting diseases [Delano & Moldawer, 2006; Slee, 2012].

The accelerated oxidative metabolism in the arthritic liver has been proposed to generate a more oxidized cellular environment which, in turn, is associated to an increased oxidative stress in the organ [Comar et al., 2013]. Under such conditions one can also expect stimulation of the catabolism of FA, a phenomenon that should, in turn, accentuate cachexia and diminish the plasma levels of TG in severe arthritis. The lower GSH/GSSG ratio in the liver of arthritic rats has been regarded as an indicator of the more oxidized state [Castro-Ghizoni et al., 2017; Comar et al., 2013]. However, the NAD(P)H/NAD(P)$^+$ ratios, which regulate directly FA metabolism, were not yet measured in the arthritic liver. Therefore, in the present study, the investigations of FA metabolism were complemented by evaluations of the redox status of the liver in terms of the NAD(P)H/NAD(P)$^+$ ratios. The experimental model was the adjuvant-induced arthritic rat. The latter is an experimental immunopathology which shares many features with severe rheumatoid arthritis and is used as a model for studying autoimmune chronic inflammation [Hegen et al., 2008]. Adjuvant-induced arthritis exhibits a strong and generalized inflammatory response associated with severe cachexia [Roubenoff, 2009]. The results of the present study should allow extrapolations for patients with severe rheumatoid arthritis.

MATERIALS AND METHODS

Materials

The liver perfusion apparatus was built in the workshops of the University of Maringá. Free Fatty Acid Quantitation Kit, fatty acid-free bovine serum albumin, enzymes and coenzymes were purchased from Sigma Chemical Co. (St. Louis, MO, USA). Labeled [1-^{14}C]octanoic acid (53 mCi·mmol^{-1}), [1-^{14}C]palmitic acid (60 mCi·mmol^{-1}), [1-^{14}C]oleic acid (54 mCi·mmol^{-1}), L-[*methyl*-^{3}H]carnitine hydrochloride (82 Ci·mmol^{-1}) and [^{14}C]sodium bicarbonate (5 mCi·mmol^{-1}) were purchased from Sigma Chemical Co. (St. Louis, MO, USA) and New England Nuclear (Boston, MA, USA). Commercial kits for the assay of triglycerides (TG), total cholesterol, HDL cholesterol and glucose were purchased from Gold Analisa Diagnóstica Ltda (Belo Horizonte, MG, Brazil). All other chemicals were of analytical grade.

Animals and induction of arthritis

Male *Holtzman* rats weighting 180-210 g (50 days old) were obtained from the Center of Animal Breeding of the State University of Maringá (UEM) and maintained under standard laboratory conditions at a temperature of 24±3ºC under a regulated 12 h light/dark cycle. The animals were housed in conventional steel cages (3 rats/cage) and fed *ad libitum* with a standard laboratory diet (Nuvilab®, Colombo, Brazil). For arthritis induction, animals were injected subcutaneously in the left hind paw with 0.1 ml (500 µg) of Freund's adjuvant (heat inactivated *Mycobacterium tuberculosis*, derived from the human strain H37Rv), suspended in mineral oil [Bracht et al., 2016]. Animals were used for experiments at day 18th after adjuvant injection. Rats of similar ages served as controls. All procedures followed the guidelines of the Brazilian Council for the Control of Animal Experimentation (CONCEA) and were previously approved by the Ethics Committee for Animal Experimentation of the State University of Maringá (Protocol number 094/2013-CEAE).

Cachexia characterization

The body weight of animals was monitored daily and the loss of body mass (LBM) was calculated as follows LBM = 100 x (BM*i* – BM*f* + GBM)/(BM*i* +

GBM), where BM*i* and BM*f* are, respectively, initial and final body mass of the arthritic rats (g). GBM is the body mass gain of the control rats after 18 days (g). Rats were considered cachectic when the LBM was higher than 10% [Fonseca et al., 2011].

Blood collection and liver homogenate preparation

Fed and 12 h fasted rats were deeply anesthetized with sodium thiopental (100 $mg \cdot kg^{-1}$) plus lidocaine (10 $mg \cdot Kg^{-1}$). The peritoneal cavity was surgically exposed and blood was collected from the cava vein and deposited into tubes with 4 mM EDTA. The liver was subsequently removed, freeze-clamped and stored in liquid nitrogen for adenine nucleotides and lipids assessment. Blood was centrifuged at 3,000*g* for10 min and the supernatant was separated as the plasma fraction.

Plasma and liver lipids and ketone bodies assays

Total lipids were extracted from the freeze-clamped livers with chloroform and methanol as previously described [Folch et al., 1957]. Total lipids were then measured by gravimetry and thereafter dissolved in a mixture of chloroform and isopropanol (1:2) for TG and cholesterol assay using commercial kits (Gold Analisa®). The results of total lipids were expressed as g per 100 g of liver weight and the results of TG and cholesterol expressed as mg per g of total lipids. TG, FFA, glycerol, total cholesterol, HDL cholesterol, acetoacetate and β-hydroxybutyrate were additionally assayed in the plasma [Bergmeyer, 1974]. LDL cholesterol and VLDL were calculated according to Friedewald's equation.

Liver perfusion

Hemoglobin-free non-recirculating liver perfusion was performed as previously described [Comar et al., 2003]. After cannulation of the portal and cava veins, the liver was removed and positioned in a plexiglass chamber. The perfusion fluid was Krebs/Henseleit-bicarbonate buffer (pH 7.4), saturated with a mixture of oxygen and carbon dioxide (95:5) by means of a membrane oxygenator with simultaneous temperature adjustment at 37 ºC. The flow was maintained constant by a peristaltic pump (Minipuls 3, Gilson, France) and it

was adjusted to between 30 and 33 $mL \cdot min^{-1}$. Oxygen concentration in the venous perfusate was monitored by a teflon-shielded platinum electrode. Samples of the effluent perfusion fluid were collected at two minutes intervals and analyzed for their metabolite content. At the end of perfusion, the liver was removed and weighed to allow precise metabolic calculations.

Activity of citric acid cycle

Livers from fed and 12 h fasted rats were perfused with Krebs/Henseleit-bicarbonate buffer. After stabilization of oxygen consumption, the livers were perfused with trace amounts of [1-^{14}C]octanoic acid (0.01 $\mu Ci \cdot mL^{-1}$) during 20 minutes. This procedure effectively measures the citric acid cycle via labelling of of the acetyl-CoA pool [Soboll et al., 1981]. The perfusate effluent was collected in Erlenmeyer flasks and carbon dioxide was measured by trapping $^{14}CO_2$ in phenylethylamine [Comar et al., 2010]. Radioactivity was measured by liquid scintillation spectrometry (TriCarb 2810 TR counter, PerkinElmer) and the results expressed as fraction of the inflowing radioactivity. The following scintillation solution was used: toluene/ethanol (2:1) containing 5 $g \cdot L^{-1}$ 2,5-diphenyloxazole and 0.15 $g \cdot L^{-1}$ 2,2-p-phenylenebis(5-phenyloxazole). Lactate and pyruvate were measured in the effluent perfused of fed rats and acetoacetate and β-hydroxybutyrate in the perfusate of fasted rats [Bergmeyer, 1974].

Net uptake rate of free fatty acids (FFA)

Livers from fed and fasted rats were perfused with Krebs/Henseleit-bicarbonate buffer. After stabilization of oxygen consumption, the livers were perfused with 0.3 mM palmitic acid or oleic acid during 10 minutes. Samples of the effluent perfusate were collected and the nonesterified FA concentration was determined using the FFA Quantification Kit from Sigma-Aldrich (CN MAK044). Quantification was done by means of a calibration curve constructed with palmitic acid. The rates of FFA uptake was calculated by subtracting the outflowing from the inflowing concentration and the results expressed as $\mu mol \cdot min^{-1} \cdot g^{-1}$.

Fatty acids (FA) oxidation

Livers from 12 h fasted rats were perfused with Krebs/Henseleit-bicarbonate buffer. After stabilization of oxygen consumption, the livers were perfused with 0.3 mM palmitic acid or oleic acid complexed with free-fatty acid bovine-serum albumin (0.15 mM) during 20 minutes. [1-^{14}C]Palmitic acid or [1-^{14}C]oleic acid (0.2 μCi·mL^{-1}) were infused. The effluent perfusate was collected in Erlenmeyer flasks and $^{14}CO_2$ trapped and measured as described for the citric acid cycle. Aliquots of the effluent perfusate were separated for measuring acetoacetate and β-hydroxybutyrate [Bergmeyer, 1974]. The results were expressed as μmol·min^{-1}·g^{-1}.

Hepatic contents of adenine nucleotides

For measuring of the acid-stable adenine nucleotides (ATP, ADP, AMP, $NADP^+$ and NAD^+), 2 g of freeze-clamped liver were macerated in liquid nitrogen and three volumes of 0.6 M perchloric acid were added to the powder tissue. The suspension was then homogenized in a van Potter-Elvehjem homogenizer and the resulting homogenate centrifuged at 4,000*g* for 10 minutes. The supernatant was neutralized with potassium carbonate, filtrated and used for nucleotides determination by high-performance liquid chromatography (HPLC) analysis.

The acid-labile NADH and NADPH were extracted as previously described [Kalhorn et al., 1985] with modifications. Briefly, 1.5 g of freeze-clamped liver was macerated in liquid nitrogen and 10 mL of ethanol was added to the powder tissue. The suspension was homogenized and 2 mL was transferred to a solution containing ethanol and 5 M KOH (99:1%). After centrifugation at 2500*g* for 5 minutes, the pellet was suspended in 1 mL of ethanol plus 2 mL of chloroform and centrifuged at 14,000*g* for 5 minutes. The aqueous phase was neutralized with 0.1 M phosphate buffer (pH 7) and centrifuged at 12,000*g* for 3 minutes. The supernatant was filtered and used for nucleotide determinations by HPLC analysis.

The HPLC system (Shimadzu, Japan) consisted of a system controller (SCL-10AVP), two pumps (model LC10ADVP), a column oven (model CTO-10AVP) and an UV– Vis detector (model SPD-10AV). A reversed-phase C18 CLC-ODS column (5 μm, 250 × 4.6 mm i.d.; Shimadzu) protected with a CLC-ODS precolumn (5 μm, 4 × 3 mm i.d.; Phenomenex), was used with a gradient from reversed-phase 0.044 M·L^{-1} phosphate buffer solution (pH 6.0) to 0.044

$M \cdot L^{-1}$ phosphate buffer solution plus methanol (1:1; pH 7.0). For acid-stable nucleotides, in percent methanol, the gradient was the following: at 0 min, 0%; at 2.5 min, 0.5%; at 5 min, 3%; at 7 min, 5%; at 8 min, 12%; at 10 min, 15%; at 12 min, 20%; at 20 min, 30%. For NADH and NADPH, the gradient was linear from 0-20 minutes ranging from 0 to 30% of methanol. The temperature was kept at 35 °C and the injection volume was 20 µL with a flow rate of 0.8 $mL \cdot min^{-1}$. Monitoring was performed spectrophotometrically at 254 nm for acid-stable nucleotides and at 340 nm for NADH and NADPH.

Identification of the peaks of investigated compounds was carried out by a comparison of their retention times with those obtained by injecting standards under the same conditions. The concentrations of the compounds were calculated by means of the regression parameters obtained from the calibration curves. The calibration curves were constructed by separating chromatographically standard solutions of the compounds. Linear relationships were obtained between the concentrations and the areas under the elution curves.

Activity of carnitine acyltransferases I and II (CAT I and II)

Firstly, rat liver mitochondria were isolated by differencial centrifugation, suspended in 5 mM Tris buffer (pH 7.2) contaning 0.1 M KCl and centrifuged at 17,000*g* for 15 minutes. The pellet was resuspended in 5 mM potassium phosphate buffer (pH 7.5) and frozen in liquid nitrogen. The extraction of the CAT I and II fractions was performed as previously described [Vicentino et al., 2002]. Both enzymes were assayed in the direction of palmitoyl-carnitine synthesis. The substrates were 0.5 mM (5 µCi/µmol) [^{3}H]carnitine and 50 µM palmitoyl-CoA. The incubation system contained 50 mM manitol, 75 mM KCl, 5% fatty acid-free bovine-serum albumin, 2 mM KCN, 25 mM EGTA, 50 µM palmitoyl-CoA and approximately 0.3 mg protein$\cdot mL^{-1}$ of either the CAT I or the CAT II preparation. The reaction (at 37 °C) was started by the addition of 0.5 mM carnitine plus 5 µCi/µmol [^{3}H]carnitine and stoped at various times (1-6 minutes) by the addition of perchloric acid. The reaction product, [^{3}H]palmitoyl-carnitine, was extracted with butanol and the radioactivity was measured by liquid scintillation spectrometry.

Activity of acetyl coenzyme A carboxylase (ACC)

The acetyl-CoA carboxylase (ACC) activity was determined by [^{14}C]sodium bicarbonate incorporation leading to the formation of [^{14}C]malonyl-CoA as previosly described [Nakanishi & Numa, 1970]. Two grams of freeze-clamped liver were macerated in liquid nitrogen and eight volumes of a medium containg 0.1 M manitol, 50 mM sodium fluoride, 10 mM Tris, 1 mM EDTA, 5 mg·L^{-1} aproptin and 5 mg·L^{-1} leupeptin. The suspension was homogenized in a van Potter-Elvehjem homogenizer and centrifuged at 48,000*g* for 20 minutes. The enzyme in the supernatant was then precipitated by the addition of 144 mg·mL^{-1} ammonium sulfate and centrifuged again at 48,000*g* for 20 minutes. The pellet was resuspended in the homogenization medium and an aliquot (0.4-0.5 mg protein) was added to a solution containing 50 mM Tris-HCl (pH 7.5), 10 mM potassium citrate, 10 mM $MgCl_2$, 3.75 mM GSH and 0.75 mg·mL^{-1} fatty acid-free bovine-serum albumin. After a pre-incubation at 37 °C for 30 minutes, the reaction was initiated (37 °C) by adding an aliquot (200 µL) of the preincubated enzyme to 0.8 ml of the assay solution containing 50 mM Tris-HCl (pH 7.5), potassium citrate up to 20 mM, 10 mM $MgCl_2$, 3.75 mM ATP, 0.125 mM acetyl-CoA, 3.75 mM GSH, 0.75 mg·mL^{-1} fatty acid-free bovine-serum albumin and 12.5 mM [^{14}C]sodium bicarbonate (4.5 nCi·mL^{-1}). After centrifugation, an aliquot of the supernatant was deposited in the cintilation flask and the remaining $^{14}CO_2$ removed in a drying oven. The Bray's scintillator solution was then added to the flask and ^{14}C measured by liquid scintillation spectrometry.

Statistical analysis

The error parameters presented in graphs and tables are standard errors of the means. Statistical analysis was done by means of the GraphPad Prism Software (version 5.0). The Student's t test was applied and the 5% level ($p < 0.05$) was adopted as a criterion of significance. Numerical analysis (initial rates of carnitine acyltransferases) was done by means of the Scientist® program from MicroMath Scientific Software.

RESULTS

Cachexia

The mean initial body weight of the animals was 214 ± 3 g. At day 18 the body weight of control and arthritic rats were 279 ± 7 g and 185 ± 2 g, respectively. In practical terms, arthritic rats did not gain body weight during this period. The loss of body mass (LBM) was 32.8 ± 0.5 % in the arthritic condition.

Lipid and ketone bodies profiles in the plasma and liver

Plasma and hepatic lipid profiles of control and arthritic rats were obtained in the fed and fasted state. The results are shown in Table I. For the fasted state, the levels of TG and total, HDL, LDL and VLDL cholesterol were approximately 20% lower and the levels of FFA and glycerol were 38% and 66% higher in the plasma of arthritic rats. The levels of acetoacetate were 280% higher and the levels of β-hydroxybutyrate and total ketone bodies were 67 and 45% lower, respectively, in the plasma of arthritic rats. These opposite effects on the acetoacetate and β-hydroxybutyrate levels produced a 11.6-fold diminution of the *β*-hydroxybutyrate/acetoacetate ratio. For the fed state, the levels of total, HDL and LDL cholesterol were 8, 19 and 13% lower in the plasma of arthritic rats. The levels of plasma TG were not affected by arthritis in the fed state, but those of FFA and glycerol were 43 and 38% higher in the arthritic condition.

Hepatic levels of total lipids, TG and total cholesterol in the fasted state were 25, 35 and 25% lower in arthritic rats. For fed state, hepatic levels of total lipids, TG and total cholesterol were 17, 36 and 19% lower in arthritic rats.

Citric acid cycle

Figure 1A illustrates the time courses of $^{14}CO_2$ production of the experiments in which trace amounts of [^{14}C]octanoate were infused in livers from fed rats in order do label the acetyl-CoA pools. The $^{14}CO_2$ production under these conditions reflects the citric acid cycle activity of livers surviving at the expense of glycogen degradation via glycolysis and oxidation of

endogenous FA [Fedatto et al., 2002]. The infusion of trace amounts of [1-^{14}C]octanoate produces no net alterations in oxygen uptake, does not affect the glycolytic flux, but effectively labels the acetyl-CoA pool. In order to compare the groups, the numerical values of each parameter at 30 minutes perfusion time in Figure 1A (steady-state) were displayed in Table II. The $^{14}CO_2$ production (citric acid cycle) was 23% higher in the livers of arthritic rats, but oxygen consumption and pyruvate production were not different. Lactate production and glycolysis were 50% higher in the livers of arthritic rats. The lactate/pyruvate ratio was 1.7-fold higher in the arthritic liver, what indicates a higher cytosolic NADH/NAD^+ ratio.

Figure 1B illustrates the time courses of $^{14}CO_2$, acetoacetate and β-hydroxybutyrate productions in the perfused livers of fasted rats upon the infusion of trace amounts of [^{14}C]octanoate. Under this condition, perfused livers survive at the expense of endogenous FA oxidation and may additionally produce ketone bodies. The numerical the steady state values are shown in Table II. $^{14}CO_2$ and β-hydroxybutyrate productions were not different, but oxygen consumption and acetoacetate production were 23 and 190% higher in the perfused livers of arthritic rats. The β-hydroxybutyrate/acetoacetate ratio was 4.8-fold lower in the arthritic condition, what indicates a very low mitochondrial NADH/NAD^+ ratio.

Hepatic uptake and oxidation of fatty acids (FA)

Figure 2 shows the net uptake rate of palmitic and oleic acids in perfused livers of fed and fasted rats. The uptake of palmitic acid was 40 and 53% higher in perfused livers of fed and fasted arthritic rats, respectively. The uptake of oleic acid was 48 and 67% higher in perfused livers of fed and fasted arthritic rats, respectively.

Figure 3 illustrates the time courses of palmitic acid (Panel A) and oleic acid (Panel B) catabolism in perfused livers of fasted control and arthritic rats. In order to compare the groups, the numerical values of each parameter at 20 minutes perfusion time in Figure 3A and B were subtracted from those values at 10 minutes perfusion time (basal rates) and displayed in Table III. The production of $^{14}CO_2$ was 46 and 80% higher in livers from arthritic rats when palmitic and oleic acid were the substrates, respectively. The increments of oxygen consumption caused by palmitic and oleic acid were 114 and 90%

higher in the arthritic condition, respectively. The acetoacetate production was also higher in the arthritic condition, 150 and 450%, respectively, with palmitic and oleic acid. The β-hydroxybutyrate, however, was lower in the arthritic condition, -46 and -58%, respectively, with palmitic and oleic acid. The sum of β-hydroxybutyrate and acetoacetate productions (total ketone bodies) was not modified by arthritis, but the β-hydroxybutyrate/acetoacetate ratio was substantially decreased, 11.6- and 11.1-fold with palmitic and oleic acid, respectively. This indicates a very low mitochondrial NADH/NAD^+ ratio in the liver of arthritic rats.

Hepatic content of adenine nucleotides

The levels of ATP, ADP, AMP, NAD^+, $NADP^+$, NADH and NADPH were quantified in the liver homogenate of control and arthritic rats. Figure 4 shows an overview of the chromatographic profile of acid-stable adenine nucleotides in the liver of fed (Panel A) and fasted (Panel B) rats. Figure 5 illustrates a typical chromatographic profile of acid-labile adenine nucleotides. Table IV shows the contents of adenine nucleotides in μmol per gram liver. Regarding the adenine mononucleotides (ATP, ADP and AMP), only the hepatic levels of ATP in the fed state were different in arthritic rats (+33%; compared to the controls). However, irrespective of being control or arthritic rats, the hepatic levels of ATP were lower and those of AMP higher in the fasted when compared to the fed state. The latter phenomenon has already been reported and has been associated to a reduced hepatic energy state that occurs due to metabolic stressors, such as fasting [Kaminsky et al., 1983].

Regarding adenine dinucleotides, the hepatic levels of NADH and NADPH were approximately 35% lower in the arthritic condition (fasted and fed rats). Hepatic levels of NAD^+ and $NADP^+$ were 14 and 38% lower in fasted arthritic rats, but not different in fed rats. The NADH/NAD^+ and NADPH/$NADP^+$ ratios were lower in the arthritic conditions in both fasted and fed rats by factors ranging from 1.31 to 1.45-fold.

Enzyme activities

As the oxidation of FA was increased in the liver of arthritic rats and considering that the major regulatory step of FA oxidation is the entry of fatty acyl-CoA into the mitochondria, the activities of carnitine acyl transferase I and

II (CAT I and II) were evaluated in mitochondria from livers of fasted rats. The time courses of palmitoyl-carnitine formation in the range up to 6 minutes are shown in Figure 6A (CAT I) and 6B (CAT II). For obtaining the initial rates of palmitoyl-carnitine formation a polynomial of the third degree was fitted to experimental curves by means of a least-squares procedure. The continuous lines in figure 6A and B were calculated with the fitted parameters and the coefficient of the first term corresponds to the initial slope (initial reaction rate), which corresponds to the initial reaction rate. No difference was found for the CAT I activity (24.1 ± 1.3 and 23.6 ± 3.3 nmol·min^{-1}·mg protein^{-1}, respectively, for control and arthritic rats). The initial rate of the CAT II activity, however, was 40% lower in the arthritic condition (33.2 ± 4.4 and 19.5 ± 0.3 nmol·min^{-1}·mg protein^{-1}, respectively, for control and arthritic rats; p=0.036).

The enzyme CAT I is negatively modulated by malonyl-CoA, which is formed as an intermediate of FA synthesis by the acetyl-CoA carboxylase (ACC). It is, thus, of interest obtain to measure its activity in order to infer about the malonyl-CoA synthesis in arthritic rats. The ACC was extracted as described in the Materials and Methods section and its activity was measured in the absence and presence of citrate at various concentrations. The latter is an allosteric activator of the ACC, whose activity also depends on the degree of phosphorylation [Beaty & Lane, 1963; Hashimoto & Numa, 1971]. The results are shown in Figure 7. In the absence of citrate the activity of ACC was lower in the arthritic state, by 27.4% ($p = 0.009$) in the fasted rats and, more modestly, by 14.7% in the fed state ($p = 0.001$). This activity corresponds to the non-phosphorylated ACC, as phosphorylation inactivates the enzyme [Beaty & Lane, 1963; Hashimoto & Numa, 1971]. It should be noted that in the absence of citrate the activity of ACC in fed rats considerably exceeds that of fasted rats. Citrate reverses inactivation by phosphorylation, a known phenomenon that was more pronounced in the fed state as illustrated by Figure 7. Activation by citrate follows Michaelian saturation kinetics [Beaty and Lane, 1963; Hashimoto and Numa, 1971], and in order to obtain quantitative parameters a Michaelis-Menten relationship was fitted to the experimental rates (v):

$$v = \frac{V_{max}[Citrate]}{[Citrate] + K_{act}} + v_o \qquad (1)$$

K_{act} is the activation constant of citrate, V_{max} corresponds to the maximal stimulation caused by citrate above the basal rate, which is represented by v_o. The continuous lines in Figure 7 were calculated by substituting the optimized parameters into equation (1). The optimized values are given in the legend to Figure 7, together with their standard errors that were quite pronounced for the data obtained in the fasted state but much smaller for the corresponding data obtained in the fed state. Arthritis did not change significantly the activation constant. It diminished, however, the maximal activation in the fed state by 19.5% ($p < 0.001$). No such change was found in the fasted state.

DISCUSSION

General aspects

The experimental model of chronic inflammation used in the present study is considered a model of severe arthritis in rats and it shares features of advanced and uncontrolled rheumatoid arthritis [Stolina et al., 2009; Hegen et al., 2008]. These animals present generalized inflammatory manifestations and severe cachexia resembling that one occurring in chronic wasting diseases, in which muscle wasting is associated to adipose tissue wasting and body weight reduction [Bracht et al., 2016; Hegen et al., 2008]. Cachexia is characterized by a loss of body mass greater than 10% associated with an underlying illness and severe cachexia occurs when the loss of body mass is higher than 15% [Evans et al., 2008]. In this study, the loss of body mass in arthritic rats was greater than 30% and it indicates severe cachexia in rats [Fonseca et al., 2011].

Before discussing the results obtained in the present study in detail it seems worth to summarize the most important findings. In arthritic rats (1) the levels of triglycerides (TG) and total cholesterol are decreased in the plasma and liver; (2) the levels of free fatty acids (FFA) and glycerol are increased whereas ketone bodies are decreased in the plasma; (3) uptake and oxidation of palmitic and oleic acids in the liver are increased; (3) ketogenesis is not modified, but the β-hydroxybutyrate/acetoacetate ratio in the liver was 85% lower; (4) the hepatic citric acid cycle activity tends to be operate at higher rates; (5) the hepatic overall NADH/NAD^+ and NADPH/$NADP^+$ ratios are lower. These events are highlighted in Figure 8, which attempts to represent in a schematic way the integrated lipid metabolism occurring in the adipose tissue and liver of arthritic rats. These events will be discussed in the following paragraphs.

Lipid and ketone bodies levels in plasma and liver of arthritic rats

In adipose tissue, proinflammatory cytokines, especially those released from the rheumatic joints, stimulate the tissue to release circulating FFA and glycerol. In this sense, rats with adjuvant-induced arthritis present reduced white adipose mass and decreased expression of fatty acid synthase (FAS) and adiponectin associated with a higher expression of TNF-α [Martin et al., 2008;

Haruna et al., 2007]. TNF-α is reported to inhibit the adipose tissue expression of FAS and ACC as well as to stimulate the expression of the hormone sensible lipase (HSL) via NFκB [Martin et al., 2008; Delano & Moldawer, 2006]. In the present study, the proposed increased lipolysis in arthritic rats is corroborated by the increased levels of circulating glycerol and FFA that were found. The increased lipolysis in the adipose tissue seems to occur even in the fed state as indicated by higher levels of FFA and glycerol in the plasma of fed arthritic rats. It should be remarked that the plasma levels of FFA were elevated in spite of their enhanced uptake by the liver. This can only occur if uptake by other tissues, such as skeletal muscle and heart muscle, for example, is diminished. In this respect it is interesting to emphasize that inflammatory stress, TNF-α and IL-1 were reported to downregulate the fatty acids translocase (FAT/CD36) expression in heart and skeletal muscle whereas upregulation was found in the liver [Wang et al., 2014; Memon et al., 1998]. FAT/CD36 is the main (long-chain) fatty acids transporter in heart and skeletal muscle [Schindler et al., 2017]. Such a combination, increased hepatic uptake of FFA and diminished uptake in peripheral tissues, has already been observed in animals lacking FAT/CD36 [Hames et al., 2014; Goudriaan et al., 2003].

High levels of circulating FFA are considered by itself proatherogenic and when further associated to high degrees of inflammation can contribute to the greater occurrence of cardiovascular disease in severe rheumatoid arthritis [Summers et al., 2010; Sattar et al., 2003]. Moreover, FFA dose-dependently enhances the secretion of proinflammatory cytokines and matrix-degrading enzymes in rheumatoid arthritis synovial fibroblasts [Frommer et al., 2015]. The lower levels of both hepatic and circulating TG in arthritic rats seem to occur as consequence of the increased FA oxidation in the liver, especially when it is associated to decreased hepatic FA synthesis and esterification. The latter condition is the opposite of what has been observed in cachexia induced by chronic wasting diseases, in which hepatic lipogenesis and circulating TG are increased [Delano & Moldawer, 2006; Slee, 2012]. The lower hepatic lipogenesis may additionally explain the reduced circulating levels of TG that occur in patients with severe rheumatoid arthritis [Zegkos et al., 2016; Myasoedova et al., 2011; Kitas & Gabriel, 2011; Choy & Sattar, 2009]. The enzyme acetyl-CoA carboxylase (ACC) catalyzes the carboxylation of acetyl-CoA to produce malonyl-CoA and it is an important regulatory step of FA

synthesis. Although only a relatively small diminution in the activity of ACC was found in the present study in the liver of fed arthritic rats, it notwithstanding represents an observation that is consistent with a diminished hepatic FA synthesis in these animals.

The hepatic metabolism of endogenous fatty acids in arthritic rats

The hepatic metabolism of FA in arthritic rats is in line with that of glucose, namely, it presents a predominance of catabolic over anabolic pathways [Castro-Ghizoni et al., 2017; Fedatto et al., 2000]. This is the opposite of what occurs in the liver of rats with Walker 256 tumour-induced cachexia. In the latter hepatic FA oxidation and ketogenesis are both diminished, with a decreased activity of CAT I and an increased derivation of fatty acyl-CoA into the esterification pathway [Siddiqui & Williams, 1989; Vicentino et al., 2002].

Concerning more specifically the FA oxidation, our data allow to differentiate the phenomenon in terms of the endogenous pools and the exogenously added substrates. The $^{14}CO_2$ productions from endogenous substrates in the substrate-free perfused liver of fasted arthritic and control rats were not different, meaning also no difference in the citric acid cycle activity. It should be remarked that perfused livers under these conditions survive mainly at the expense of the oxidation of exogenous fatty acids. Oxygen consumption and ketogenesis, however, were higher in livers from arthritic fasted rats. Both phenomena can be regarded as evidence of an enhanced endogenous fatty acids oxidation. In fact, breaking down of fatty acids into acetyl-CoA is coupled to the production of reducing equivalents that are oxidized in the respiratory chain, what justifies the increased oxygen uptake. No increment in the activity of the citric acid cycle, however will occur if the resulting extra acetyl-CoA units are deviated into ketogenesis. It is true that ketone bodies are produced not only from acetyl-CoA derived from endogenous FA, but also from acetoacetyl-CoA derived from the oxidation of ketogenic amino acids. The latter occurs mainly under extreme conditions in which skeletal muscle wasting is involved, such as severe cachexia [Grabacka et al., 2016]. Thus, in substrate-free perfused livers from fasted rats it is more likely that the extra ketogenesis in the arthritic condition represents increased oxidation of both fatty acids and amino acids.

In substrate-free perfused livers from fed rats, on the other hand, the activity of the citric acid cycle was somewhat higher in the arthritic condition (+23%) and oxygen uptake presented merely a tendency toward higher values. These relatively modest differences reflect most likely the differences in metabolic state. Substrate-free perfused livers from fed rats do not depend solely on the oxidation of endogenous fatty acids. Actually, the glycolytic activity, that is enhanced in the arthritic state [Castro-Ghizoni et al., 2017; Fedatto et al., 2000], leads by itself to the production of reducing equivalents and acetyl-CoA from pyruvate. Glycolysis is one of the reasons why substrate-free perfused livers from fed rats produce much less ketone bodies [Scholz et al., 1984]. It is thus likely that the oxidation of endogenous fatty acids in substrate-free perfused livers from arthritic rats was only modestly increased or even not increased at all. The increased flux of glucose through glycolysis in the arthritic condition, may explain at least in part, the higher ATP content in the liver of fed arthritic rats.

At this point it is important to note that the higher rates of ketogenesis described here are in contrast to the lower levels of circulating ketone bodies in the arthritic condition. This may be an apparent contradiction, however, because there is evidence indicating an increased uptake by peripheral tissues in arthritis. Ketone bodies are avidly absorbed from blood in the peripheral tissues by the monocarboxylate transporter 1 (MCT1), which is expressed in virtually every cell [Grabacka et al., 2016]. Moreover, TNF-α and IL-1 stimulate PPAR-γ coactivator-1 alpha (PGC-1α), which upregulates MCT1 in skeletal muscle [Benton et al., 2008; Puigserver et al., 2001].

The hepatic metabolism of exogenously supplied fatty acids in arthritic rats

The higher rates of uptake of FFA in the perfused livers of arthritic rats occurs in both fed and fasted states and reflects their higher oxidation in the organ. This is because the driving force governing FFA uptake is the metabolic demand for them and it is generally accepted that conversion of FA into acyl-CoA and downstream metabolic intermediates increases cellular FFA uptake [Mashek & Coleman, 2006]. In vivo, however, the hepatic uptake of FFA is possibly even more increased than in the perfused liver due to their higher circulating levels in arthritis and because the liver extracts these substrates in proportion their concentration in blood [Ferraresi-Filho et al., 1992; Frayn et

al., 2006]. It should be noted that in accordance to previous studies [Ferraresi-Filho et al., 1992; Mito et al., 2010] palmitic acid uptake was more pronounced than oleic acid uptake in both control and arthritic rats.

The oxygen consumption increments and the $^{14}CO_2$ productions from exogenous FA were more elevated in the liver of arthritic rats, but the increments in ketogenesis were not modified (Table III). Although the increment in ketogenesis caused by exogenous FA was not different, the β-hydroxybutyrate/acetoacetate ratio was lower in arthritic rats. This occurs when the near-equilibrium of the 3-hydroxybutyrate dehydrogenase reaction is shifted toward acetoacetate, a condition that reflects a lower NADH/NAD^+ ratio [Robinson & Williamson, 1980]. The latter was actually decreased in the liver of arthritic rats (Table IV). Moreover, the same phenomenon also stimulates the citric acid cycle by shifting the near-equilibrium of the malate dehydrogenase reaction in the direction of oxaloacetate, the acceptor of acetyl-CoA in the cycle [Vicentino et al., 2002]. The lower β-hydroxybutyrate/acetoacetate ratio in the mitochondria of arthritic rats correlates well with the same phenomenon in the plasma. In this respect it should be noted that monocarboxylates are rapidly transported into and out of the cells by MCT1 so that their extracellular concentration ratio in blood matches their intracellular concentration ratio [Halestrap & Wilson, 2012].

The more oxidized state found in the liver of arthritic rats deserves a few additional comments. In the present study, the hepatic contents of adenine nucleotides were directly measured and they reflect their mean concentrations over the total tissue without informing about their distribution in the various cell compartments. However, the lower β-hydroxybutyrate/acetoacetate ratio observed in the perfused livers from arthritic rats indicates a lower mitochondrial NADH/NAD^+ ratio. The same was found previously for the hepatocyte cytosol of fasted arthritic rats [Fedatto et al., 2000]. In the fed state, however, the higher lactate/pyruvate ratio indicates a higher cytosolic NADH/NAD^+ ratio in the arthritic liver. The latter was found even under net oxidizing conditions in the total hepatic tissue and it occurs probably due to a higher contribution of mitochondrial oxidizing equivalents. The cytosolic redox state, however, depends not only on the NADH/NAD^+ couple, but also on the NADPH/$NADP^+$ couple. The latter is apparently decreased in the cytosol of

arthritic rats due to the pronounced oxidative stress in the organ [Comar et al., 2013].

The increased oxidation of FA in the liver of arthritic rats found in this work was not paralleled by an increased activity of CAT I and CAT II, the enzymes responsible for shuttling the fatty acid moieties into the mitochondria. For CAT I even the opposite was found, i.e., its activity measured under standardized conditions was higher in healthy rats. There is evidence, however, that the ACC catalyzed production of malonyl-CoA, the negative modulator of CAT I, could be diminished in arthritic fed rats, especially in the presence of citrate, so that one cannot exclude the possibility that the actual CAT I activity was increased in the liver cells of arthritic fed rats. In support to this view is the general notion that, in the fasted state, the mitochondrial oxidation of FA is greatly favored because the formation of malonyl-CoA is very low [McGarry & Foster, 1980]. Irrespective of the participation or not of the CAT I activity in the increased rates of hepatic FA oxidation in arthritic rats, the crucial role of the more oxidized state of the mitochondrial NADH-NAD^+ couple can hardly be overemphasized, as the higher NAD^+ concentrations are an important factor in determining the reaction rate of dehydrogenases in general. Furthermore, the lower cytosolic NADPH/$NADP^+$ ratio in arthritic livers is also likely to contribute to decrease the FA synthesis.

The redox potential of the NADH-NAD^+ and NADPH-$NADP^+$ couples and oxidative stress

The reason by which the NADH-NAD^+ and NADPH-$NADP^+$ couples are shifted toward an oxidized state in the arthritic liver has not yet been completely clarified, but it has been attributed to the pronounced oxidative stress associated to the accelerated oxidative metabolism in the organ [Comar et al., 2013]. The altered oxidative stress is consequence of an impaired antioxidant system associated to an increased production of ROS, both mediated by inflammatory cytokines. The pronounced oxidative stress consumes an excessive amount of reducing equivalents to unsuccessfully neutralize the more intense ROS production and, therefore, to decrease the NADPH/$NADP^+$ ratio in the liver of arthritic animals [Comar et al., 2013]. The higher oxygen consumption in arthritic livers (Table II and Figure 2) corroborates the accelerated oxidative metabolism. In addition, TNF-α has been

reported to induce mitochondrial oxygen consumption by uncoupling respiration in liver cells [Kastl et al., 2014]. Therefore, pro-inflammatory cytokines may be increasing the FA oxidation by accelerating mitochondrial oxygen consumption and by modifying via oxidative stress the redox status of the arthritic liver.

Concluding remarks

In conclusion, the results of the present study reveal that the levels of circulating free fatty acids (FFA) are increased in arthritic rats, possibly a consequence of cytokine-induced adipose tissue lipolysis. Uptake and oxidation of FFA are increased in the liver of arthritic rats and seem to be consequence of a more oxidized state associated with an accelerated mitochondrial oxidative metabolism accompanied by a pronounced oxidative stress. This increased oxidation of fatty acids is likely to contribute to the lower levels of circulating and hepatic triglycerides (TG) a phenomenon that may also be enhanced by a diminished biosynthesis. These results reveal that, as opposed to other chronic wasting diseases, the lipid hepatic metabolism in arthritic rats is shifted toward a catabolic state. Such a condition certainly contributes to the marked cachexia verified in rats with adjuvant-induced arthritis and possibly in patients with severe rheumatoid arthritis.

Acknowledgements

Authors wish to thank the financial support of the Coordenação de Aperfeiçoamento de Pessoal de Nível Superior (CAPES) and of the Conselho Nacional de Desenvolvimento Científico e Tecnológico (CNPq).

Competing interests

The authors declare that no competing interest exists and that all approved the final manuscript.

Authors' contributions

JFC conceived and designed the experiments. CABA induced the arthritis. MMNW, GBFS, AVP and LSC performed the experiments. JFC wrote the paper. AB reviewed the paper. All authors have read and approved the final version of the paper.

REFERENCES

Beaty NB, Lane MD, 1983. Kinetics of activation of acetyl-CoA carboxylase by citrate. J Biol Chem 258:13043-1350. http://dx.doi.org/

Benton CR, Yoshida Y, Lally J, Han XX, Hatta H, Bonen A. 2008. PGC-1alpha increases skeletal muscle lactate uptake by increasing the expression of MCT1 but not MCT2 or MCT4. Physiol Genomics 35:45-54. http://dx.doi.org/10.1152/physiolgenomics.90217.2008

Bergmeyer HU. 1974. Methods of Enzymatic Analysis. London:Verlag Chemie-Academic Press. ISBN:352725370X, 9783527253708

Bracht A, Silveira SS, Castro-Ghizoni CV, Sá-Nakanishi AB, Oliveira MRN, Bersani-Amado CA, Peralta RM, Comar JF. 2016. Oxidative changes in the blood and serum albumin differentiate rats with monoarthritis and polyarthritis. SpringerPlus 5:36-50. http://dx.doi.org/10.1186/s40064-016-1671-1

Castro-Ghizoni CV, Ames APA, Lameira OA, Bersani-Amado CA, Sá-Nakanishi AB, Bracht L, Natali MRM, Peralta RM, Bracht A, Comar JF. 2017. Anti-inflammatory and antioxidant actions of copaiba oil (*Copaifera reticulata*) are associated with histological modifications in the liver of arthritic rats. J Cell Biochem 118:3409-3423. http://dx.doi.org/10.1002/jcb.25998

Choy E, Ganeshalingam K, Semb AG, Szekanecz Z, Nurmohamed M. 2014. Cardiovascular risk in rheumatoid arthritis: recent advances in the understanding of the pivotal role of inflammation, risk predictors and the impact of treatment. Rheumatology 53:2143–2154. https://dx.doi.org/10.1093/rheumatology/keu224

Choy E, Sattar N. 2009. Interpreting lipid levels in the context of high-grade inflammatory states with a focus on rheumatoid arthritis: a challenge to conventional cardiovascular risk actions. Ann Rheum Dis 68:460-469. http://dx.doi.org/10.1136/ard.2008.101964

Comar JF, Sá-Nakanishi AB, Oliveira AL, Wendt MMN, Bersani-Amado CA, Ishii-Iwamoto EL, Peralta RM, Bracht A. 2013. Oxidative state of the liver of rats with adjuvant-induced arthritis. Free Rad Biol Med 58:144-153. https://doi.org/10.1016/j.freeradbiomed.2012.12.003

Comar JF, Suzuki-Kemmelmeier F, Constantin J, Bracht A. 2010. Hepatic zonation of carbon and nitrogen fluxes derived from glutamine and ammonia transformations. J Biomed Sci 17:1. http://dx.doi.org/10.1186/1423-0127-17-1

Comar JF, Suzuki-Kemmelmeier F, Bracht A. 2003. The action of oxybutinin on haemodynamics and metabolism in the perfused rat liver. Basic Clin Pharmacol Toxicol 93:147-152. http://dx.doi.org/10.1034/j.1600-0773.2003.930307.x

Delano MJ, Moldawer LL. The Origins of Cachexia in Acute and Chronic Inflammatory Diseases. 2006. Nutr Clin Pract 21:68-81. http://dx.doi.org/10.1177/011542650602100168

Emmison N, Agius L. 1988. Fatty acid uptake and metabolism to ketone bodies and triacylglycerol in rat and human hepatocyte cultures is dependent on chain-

length and degree of saturation: effects of carnitine and glucagon. FEBS Letters 236:83-88. https://doi.org/10.1016/0014-5793(88)80289-8

Evans WJ, Morley JE, Argilés J, Bales C, Baracos V, Guttridge D, Jatoi A, Kalantar-Zadeh K, Lochs H, Mantovani G, Marks D, Mitch WE, Muscaritoli M, Najand A, Ponikowski P, Fanellia FR, Schambelan M, Schols A, Anker SD. 2008. Cachexia: a new definition. Clin Nutr 27:793-799. https://doi.org/10.1016/j.clnu.2008.06.013

Fedatto Jr Z, Ishii-Iwamoto EL, Caparroz-Assef SM, Vicentini GE, Bracht A, Kelmer-Bracht AM. 2002. Glycogen levels and glycogen catabolism in livers from arthritic rats. Mol Cell Biochem 229:1-7. http://dx.doi.org/10.1023/A:1017913124084

Fedatto Jr Z, Ishii-Iwamoto EL, Amado CB, Maciel ERM, Bracht A, Kelmer-Bracht AM. 2000. Glucose phosphorylation capacity and glycolysis in the liver of arthritic rats. Inflamm Res 49:128-132. http://dx.doi.org/10.1007/s000110050570

Ferraresi-Filho O, Ferraresi ML, Constantin J, Ishii-Iwamoto EL, Schwab AJ, Bracht A. 1992. Transport and metabolism of palmitate in the rat liver. Net flux and unidirectional fluxes across the cell membrane. Biochim Biophys Acta Biomembranes 1103:239-249. https://doi.org/10.1016/0005-2736(92)90093-2

Folch J, Lees M, Sloane-Stanley GH. 1957. A simple method for the isolation and purification of total lipides from animal tissues. J Biol Chem 226:497-509.

Fonseca EAI, Oliveira MA, Lobato NS, Akamine EH, Colquhoun A, Carvalho MHC, Zyngier SB, Fortes ZB. 2011. Metformin reduces the stimulatory effect of obesity on in vivo Walker-256 tumor development and increases the area of tumor necrosis. Life Sci 88:846-852. https://doi.org/10.1016/j.lfs.2011.03.005

Frayn KN, Arner P, Yki-Järvinen H. 2006. Fatty acid metabolism in adipose tissue, muscle and liver in health and disease. Essays Biochem 42:89-103. http://dx.doi.org/10.1042/bse0420089

Frommer KW, Schäffler A, Rehart S, Lehr A, Müller-Ladner U, Neumann E. 2015. Free fatty acids: potential proinflammatory mediators in rheumatic diseases. Ann Rheum Dis 74:303-310. http://doi.org/10.1136/annrheumdis-2013-203755

Gonzalez-Gay MA, Gonzalez-Juanatey C, Martin J. 2005. Rheumatoid Arthritis: A Disease Associated with Accelerated Atherogenesis. Sem Arthr Rheum 35:8-17. https://dx.doi.org/10.1016/j.semarthrit.2005.03.004

Goudriaan JR, Dahlmans VE, Teusink B, Ouwens DM, Febbraio M, Maassen JA, Romijn JA, Havekes LM, Voshol PJ. 2003. CD36 deficiency increases insulin sensitivity in muscle, but induces insulin resistance in the liver in mice. J Lipid Res 44:2270-2277. https://dx.doi.org/10.1194/jlr.M300143-JLR200

Hashimoto T, Numa S. 1971. Kinetic studies on the reaction mechanism and the citrate activation of liver acetyl coenzyme A carboxylase. Eur J Biochem 18:319-331. https://dx.doi.org/10.1111/j.1432-1033.1971.tb01247.x

Grabacka M, Pierzchalska M, Dean M, Reiss K. 2016. Regulation of Ketone Body Metabolism and the Role of PPARα. Int J Mol Sci 17:2093. https://dx.doi.org/10.3390/ijms17122093

Halestrap AP, Wilson MC. 2012. The monocarboxylate transporter family-Role and regulation. IUBMB Life 64:109-119. https://dx.doi.org/10.1002/iub.572

Hames KC, Vella A, Kemp BJ, Jensen MD. 2014. Free fatty acid uptake in humans with CD36 deficiency. Diabetes 63:3606-3614. http://doi.org/10.2337/db14-0369

Haruna Y, Morita Y, Yada T, Satoh M, Fox DA, Kashihara N. 2007. Fluvastatin reverses endothelial dysfunction and increased vascular oxidative stress in rat adjuvant-induced arthritis. Arthr Rheum 56:1827–1835. https://dx.doi.org/10.1002/art.22632

Hegen M, Keith Jr JC, Collins M, Nickerson-Nutter CL. 2008. Utility of animal models for identification potential therapeutics for rheumatoid arthritis. Ann Rheum Dis 67:1505-1515. http://dx.doi.org/10.1136/ard.2007.076430

Kalhorn TF, Thummel KE, Nelson SD, Slattery JT. 1985. Analysis of oxidized and reduced pyridine dinucleotides in rat liver by high-performance liquid chromatography. Anal Biochem 151:343-7.

Kaminsky YG, Kosenko EA, Kondrashova MN. 1983. Alteration of adenine nucleotide pool in old rat liver and its normalization with ammonium succinate. FEBS Lett 159:259-261. https://doi.org/10.1016/0014-5793(83)80459-1

Kastl L, Sauer SW, Ruppert T, Beissbarth T, Becker MS, Süss D, Krammer PH, Gülow K. 2014. TNF-α mediates mitochondrial uncoupling and enhances ROS-dependent cell migration via NF-κB activation in liver cells. FEBS Lett 588:175-183. https://doi.org/10.1016/j.febslet.2013.11.033

Khovidhunkit W, Memon RA, Feingold KR, Grunfeld C. 2000. Infection and inflammation-induced proatherogenic changes of lipoproteins. J Infect Dis 181:S462–S472. https://dx.doi.org/10.1086/315611

Kitas GD, Gabriel SE. 2011. Cardiovascular disease in rheumatoid arthritis: state of the art and future perspectives. Ann Rheum Dis 70:8-14.

Lee B, Shao J. 2012. Adiponectin and lipid metabolism in skeletal muscle. Acta Pharm Sin B 2:335-340. https://doi.org/10.1016/j.apsb.2012.06.008

Luiken JJFP, Chanda D, Nabben M, Neumann D, Glatz JFC. 2016. Post-translational modifications of CD36 (SR-B2): Implications for regulation of myocellular fatty acid uptake. Biochim Biophys Acta Mol Bas Dis 1862:2253-2258. https://doi.org/10.1016/j.bbadis.2016.09.004

Martín AI, Castillero E, Granado M, López-Menduiña M, Villanúa MA, López-Calderón A. 2008. Adipose tissue loss in adjuvant arthritis is associated with a decrease in lipogenesis, but not with an increase in lipolysis. J Endocrinol 197:111-119. http://dx.doi.org/ 10.1677/JOE-07-0491

Mashek DG, Coleman RA. 2006. Cellular fatty acid uptake: the contribution of metabolism. Curr Opin Lipidol 17:274-278. http://dx.doi.org/10.1097/01.mol.0000226119.20307.2b

Mazuko K. 2014. Rheumatoid cachexia revisited a metabolic co-morbidity in rheumatoid arthritis. Front Nutr 1:20. http://dx.doi.org/10.3389/fnut.2014.00020

McInnes IB, Schett G. 2011. The pathogenesis of rheumatoid arthritis. N Engl J Med365:2205-2209. http://dx.doi.org/10.1056/NEJMra1004965

Memon RA, Feingold KR, Moser AH, Fuller J, Grunfeld C. 1998. Regulation of fatty acid transport protein and fatty acid translocase mRNA levels by endotoxin and cytokines. Am J Physiol Endocrinol Metab 274:E210-E217. https://doi.org/10.1152/ajpendo.1998.274.2.E210

Misko TP, Radabaugh MR, Highkin M, Abrams M, Friese O, Gallavan R, Bramson C, Hellio Le Graverand MP, Lohmander LS, Roman D. 2013. Characterization of nitrotyrosine as a biomarker for arthritis and joint injury. Osteoarthritis Cart 21:151-156.

Mito MS, Constantin J, Castro CV, Yamamoto NS, Bracht A. 2010. Effects of ranolazine on fatty acid transformation in the isolated perfused rat liver. Mol Cell Biochem 345:35-44. https://doi.org/10.1007/s11010-010-0557-8

Munro R, Morrison E, McDonald AG, Hunter JA, Madhok R, Capell HA. 1997. Effect of disease modifying agents on the lipid profiles of patients with rheumatoid arthritis. Ann Rheum Dis 56:374-377. http://dx.doi.org/10.1136/ard.56.6.374

Myasoedova E, Crowson CS, Kremers HM, Roger VL, Fitz-Gibbon PD, Therneau TM, Gabriel SE. 2011. Lipid paradox in rheumatoid arthritis: the impact of serum lipid measures and systemic inflammation on the risk of cardiovascular disease. Ann Rheum Dis 70:482-487. http://dx.doi.org/10.1136/ard.2010.135871

Nakanishi S, Numa S. 1970. Purification of Rat Liver Acetyl Coenzyme A Carboxylase and Immunochemical Studies on its Synthesis and Degradation. Eur J Biochem 16:161-173. http://dx.doi.org/10.1111/j.1432-1033.1970.tb01068.x

Puigserver P, Rhee J, Lin J, Wu Z, Yoon JC, Zhang CY, Krauss S, Mootha VK, Lowell BB, Spiegelman BM. Cytokine Stimulation of Energy Expenditure through p38 MAP Kinase Activation of PPARγ Coactivator-1. Mol Cell 8:971-982. https://doi.org/10.1016/S1097-2765(01)00390-2

Robertson J, Peters MJ, McInnes IB, Sattar N. 2013. Changes in lipid levels with inflammation and therapy in RA: a maturing paradigm. Nat Rev Rheumatol 9:513-523. http://dx.doi.org/10.1038/nrrheum.2013.91

Robinson AM, Williamson DH. 1980. Physiological roles of ketone bodies as substrates and signals in mammalian tissues. Physiol Rev 60:143-187. http://dx.doi.org/10.1152/physrev.1980.60.1.143

Roubenoff R. 2009. Rheumatoid cachexia: a complication of rheumatoid arthritis moves into the 21st century. Arthritis Res Ther 11:108-109. http://dx.doi.org/10.1186/ar2658

Sattar N, Mccarey DW, Capell H, McInnes IB. 2003. Explaining how "high-grade" systemic inflammation accelerates vascular risk in rheumatoid arthritis. Circulation 108:2957-2963. https://dx.doi.org/10.1161/01.CIR.0000099844.31524.05

Schindler M, Pendzialek M, Grybel KJ, Seeling T, Gürke J, Fischer B, Navarrete Santos A. 2017. Adiponectin stimulates lipid metabolism via AMPK in rabbit blastocysts. Hum Reprod 32:1382-1392. http://doi.org/ 10.1093/humrep/dex087

Scholz R, Schwabe, Soboll S, 1984. Influence of fatty acids on energy metabolism. 1. Stimulation of oxygen consumption, ketogenesis and CO_2 production following addition of octanoate and oleate in perfused rat liver. Eur J Biochem 141:223-230. https://dx.doi.org/10.1111/j.1432-1033.1984.tb08179.x

Siddiqui RA, Williams JF. 1989. The regulation of fatty acid and branched-chain amino acid oxidation in cancer cachectic rats: A proposed role for a cytokine, eicosanoid, and hormone trilogy. Biochem Med Metabol Biol 42:71-86. https://doi.org/10.1016/0885-4505(89)90043-1

Slee AD. 2012. Exploring metabolic dysfunction in chronic kidney disease. Nutr Metab 201:29-36. https://dx.doi.org/10.1186/1743-7075-9-36

Soboll S, Heldt HW, Scholz R. 1981. Changes in the Subcellular Distribution of Metabolites Due to Ethanol Oxidation in the Perfused Rat Liver. Hoppe-Seyler's Zeitschrift für physiologische Chemie 362:247-60. http://dx.doi.org/10.1515/bchm2.1981.362.1.247

Stolina M, Bolon B, Middleton S, Dwyer D, Brown H, Duryea D, Zhu L, Rohner A, Pretorius J, Kostenuik P, Feige U, Zack D. 2009. The evolving systemic and local biomarker milieu at different stages of disease progression in rat adjuvant-induced arthritis. J Clin Immunol 29:158-174. http://dx.doi.org/10.1007/s10875-008-9238-8

Summers GD, Metsios GS, Stavropoulos-Kalinoglou A, Kitas GD. 2010. Rheumatoid cachexia and cardiovascular disease. Nat Rev Rheumatol 6:445-51. http://dx.doi.org/10.1038/nrrheum.2010.105

von Haehling S, Anker SD. 2014. Prevalence, incidence and clinical impact of cachexia: facts and numbers. J Cachexia Sarcopenia Muscle 5:261-63. http://dx.doi.org/10.1007/s13539-014-0164-8

Vicentino C, Constantin J, Bracht A, Yamamoto NS. 2002. Long-chain fatty acid uptake and oxidation in the perfused rat liver of Walker-256 tumor-bearing rats. Liver Int 22:342-350. http://dx.doi.org/10.1034/j.1600-0676.2002.01656.x

Wang C, Hu L, Zhao L, Yang P, Moorhead JF, Varghese Z, Chen Y, Ruan XZ. 2014. Inflammatory stress increases hepatic CD36 translational efficiency via activation of the mTOR signalling pathway. PLoS One 9:e103071. http://doi.org/10.1371/journal.pone.0103071

Zegkos T, Kitas G, Dimitroulas T. 2016. Cardiovascular risk in rheumatoid arthritis: assessment, management and next steps. Ther Adv Musculoskelet Dis 8:86-101. http://dx.doi.org/10.1177/1759720X16643340

Table I. ***Lipid and ketone bodies profiles in the plasma and liver of control and arthritic rats.*** The levels of lipids and glycerol were assessed in fed and 12 h fasted rats. The levels of ketone bodies were assessed only in fasted rats. The values are the mean ± standard error of six animals for each experimental condition. Pairs of values in the same line labeled with superscripts are statistically different: $^{\#}p<0.05$, $^{*}p<0.01$; ** $p<0.001$.

Plasma	Fasted		Fed	
	Control	Arthritis	Control	Arthritis
Triglycerides (TG; $mg \cdot dL^{-1}$)	75.1 ± 3.7	59.3 ± 2.0*	73.9 ± 3.8	78.1 ± 1.5
Total cholesterol ($mg \cdot dL^{-1}$)	95.8 ± 4.3	73.8 ± 3.8*	97.2 ± 1.1	89.3 ± 1.1**
HDL cholesterol ($mg \cdot dL^{-1}$)	14.1 ± 0.9	11.3 ± 0.6$^{\#}$	17.0 ± 0.9	13.8 ± 0.4*

LDL cholesterol (mg·dL^{-1})	67.6 ± 3.2	51.0 ± 3.3$^{\#}$	-------	-------
VLDL cholesterol (mg·dL^{-1})	15.0 ± 0.7	11.9 ± 0.4*	-------	-------
Free Fatty Acids (FFA; μM)	89.5 ± 3.5	123.4 ± 5.2*	40.0 ± 2.3	57.3 ± 2.8*
Glycerol (μM)	44.8 ± 3.4	74.2 ± 4.2*	26.0 ± 3.1	36.2 ± 2.2$^{\#}$
β-Hydroxybutyrate (μM)	314.8 ± 9.9	105.8 ± 4.8**	-------	-------
Acetoacetate (μM)	20.8 ± 2.8	80.6 ± 7.8*	-------	-------
Total ketone bodies (μM)	335.6 ± 8.9	186.4 ± 3.9*	-------	-------
β-Hydroxybutyrate/ acetoacetate	16.2 ± 2.9	1.4 ± 0.2**	-------	-------
Liver				
Total Lipids (g·100g liver^{-1})	4.0 ± 0.2	3.0 ± 0.1$^{\#}$	2.9 ± 0.1	2.4 ± 0.1$^{\#}$
Plasma	Fasted		Fed	
Total cholesterol (mg·g total lipids^{-1})	106.6 ± 5.8	80.4 ± 3.5$^{\#}$	72.0 ± 2.4	58.5 ± 2.4$^{\#}$

Table II. ***Citric acid cycle, glycolysis and ketogenesis from endogenous substrates in perfused rat livers.*** The livers of fed and fasted rats were perfused with Krebs/Henseleit buffer and trace amounts of [^{14}C]octanoate (0.01 μCi·mL^{-1}) as shown in Figure 1. Values are the rates of each parameter at 30 minutes perfusion time in Figure 1 (steady-state). Citric acid cycle was inferred from the $^{14}CO_2$ production and oxygen consumption; glycolysis was expressed as pyruvate + lactate production (fed rats); and ketogenesis was expressed as acetoacetate + β-hydroxybutyrate production (fasted rats). Data are the mean ± standard error of four animals for each experimental condition. Pairs of values in the same line labeled with superscripts are statistically different: $^{\#}p<0.05$, $^{*}p<0.01$, $^{**}p<0.001$.

	Control	Arthritis	Control	Arthritis
$^{14}CO_2$ production (fraction of inflow)	0.27 ± 0.01	0.27± 0.03	0.30 ± 0.01$^{\#}$	0.37 ± 0.01$^{\#}$
Oxygen Consumption ($\mu mol \cdot min^{-1} \cdot g^{-1}$)	1.92± 0.16	2.36 ±0.04$^{\#}$	1.44 ± 0.01	1.61 ± 0.08
Lactate production ($\mu mol \cdot min^{-1} \cdot g^{-1}$)	-------	-------	0.73 ± 0.13	1.12 ± 0.14$^{\#}$
Pyruvate production ($\mu mol \cdot min^{-1} \cdot g^{-1}$)	-------	-------	0.20 ± 0.03	0.17 ± 0.04
Glycolysis	-------	-------	0.82 ± 0.05*	1.28 ± 0.20*

Parameter	Palmitic acid		Oleic acid	
	Control	Arthritis	Control	Arthritis
Acetoacetate production ($\mu mol \cdot min^{-1} \cdot g^{-1}$)	0.13 ± 0.02	0.38 ± 0.01$^{\#}$	-------	-------
β-Hydroxybutyrate production ($\mu mol \cdot min^{-1} \cdot g^{-1}$)	0.03 ± 0.01	0.02 ± 0.01	-------	-------
Ketogenesis ($\mu mol \cdot min^{-1} \cdot g^{-1}$)	0.16 ± 0.02	0.40 ± 0.01**	-------	-------
β-Hydroxybutyrate/ acetoacetate	0.24 ± 0.06	0.05 ±0.01$^{\#}$	-------	-------

Table III. ***Fatty acids catabolism in perfused livers of control and arthritic rats.*** Livers of fasted rats were perfused with 0.3 mM fatty acids (palmitic and oleic acids) plus trace amounts of the corresponding [1-^{14}C]fatty acid (0.2 $\mu Ci \cdot mL^{-1}$). The values are the increment (Δ) in the rate of each parameter due to fatty acid infusion (values at 20 minutes – values at 10 minutes perfusion time in Figure 3). Ketogenesis is the sum of β-hydroxybutyrate and acetoacetate productions. Data are the mean ± standard error of three animals for each experimental condition. Pairs of values in the same line labeled with superscripts are statistically different: $^{\#}p<0.05$, $^{*}p<0.01$, $^{**}p<0.001$.

$^{14}CO_2$ production (μmol·min^{-1}·g^{-1})	0.99±0.11	1.45±0.06$^{\#}$	0.87±0.11	1.57±0.14$^{\#}$
ΔOxygen consumption (μmol·min^{-1}·g^{-1})	0.49±0.14	1.05±0.11$^{\#}$	0.22±0.04	0.42±0.06$^{\#}$
Δβ-Hydroxybutyrate production (μmol·min^{-1}·g^{-1})	0.41±0.01	0.22±0.01*	0.33±0.06	0.14±0.01$^{\#}$
ΔAcetoacetate production (μmol·min^{-1}·g^{-1})	0.11±0.01	0.27±0.03*	0.04±0.01	0.23±0.05$^{\#}$

Parameter	Fasted		Fed	
	Control	Arthritis	Control	Arthritis
acetoacetate				
ATP	1.22 ± 0.06	1.36 ± 0.08	2.03 ± 0.10	2.71 ± 0.10$^{\#}$

Table IV. **The levels of adenine mono- and dinucleotides in the liver of control and arthritic rats.** Acid-stable and acid-labile adenine nucleotides were extracted from freeze-clamped livers of fed and fasted rats and measured by HPLC (see Methods sections). The values are expressed as μmol·(g fresh liver)$^{-1}$ and data are the mean ± standard error of five animals for each experimental condition. Pairs of values in the same line labeled with superscripts are statistically different: $^{\#}p<0.05$, $^{*}p<0.01$, $^{**}p<0.001$.

ADP	1.17 ± 0.03	1.16 ± 0.04	0.81 ± 0.04	0.83 ± 0.04
AMP	1.11 ± 0.10	1.02 ± 0.04	0.39 ± 0.03	0.37 ± 0.02
$NADP^+$	0.13 ± 0.01	0.08 ± 0.01*	0.13 ± 0.02	0.11 ± 0.01
NAD^+	0.44 ± 0.02	0.38 ± 0.01$^\#$	0.47 ± 0.02	0.45 ± 0.01
NADPH	0.38 ± 0.02	0.24 ± 0.01**	0.37 ± 0.01	0.23 ± 0.01**
NADH	0.11 ± 0.01	0.07 ± 0.01$^\#$	0.09 ± 0.004	0.06 ± 0.003$^\#$
Ratios				
ATP/ADP	1.05 ± 0.04	1.17 ± 0.04	2.71 ± 0.21	3.40 ± 0.05*
ATP/AMP	1.85 ± 0.07	1.34 ± 0.07	5.99 ±0.67	7.74 ± 0.37$^\#$
$NADPH/NADP^+$	3.48 ± 0.25	2.53 ±0.21$^\#$	3.26 ±0.27	2.25 ±0.13$^\#$
$NADH/NAD^+$	0.25 ± 0.02	0.19 ± 0.02$^\#$	0.19 ± 0.02	0.14 ± 0.01$^\#$

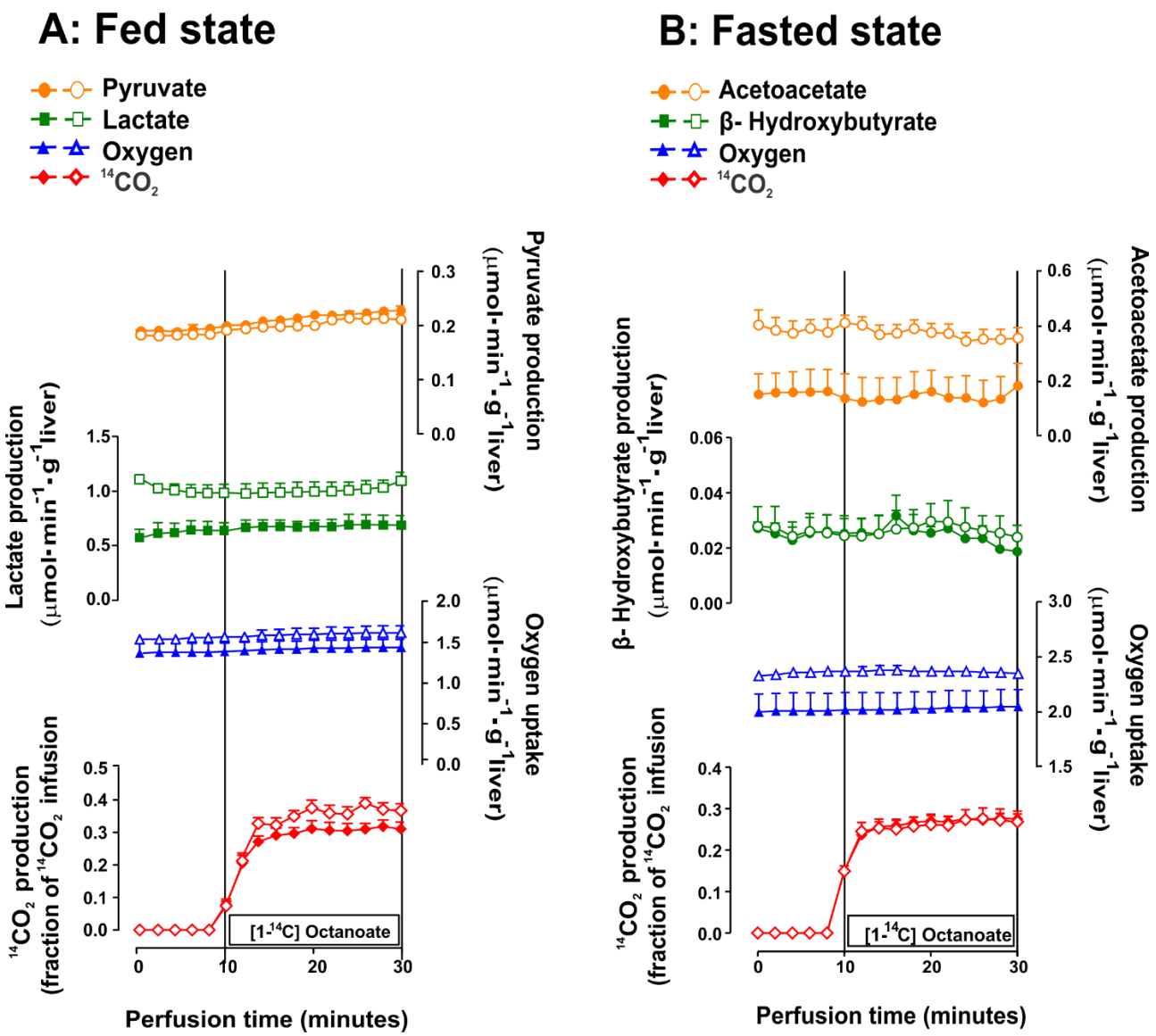

Figure 1: Citric acid cycle activity, glycolysis and ketogenesis in perfused livers from control and arthritic rats. A: Citric acid cycle and glycolysis in the liver of fed rats. **B:** Citric acid cycle and ketogenesis in the livers of fasted rats. Livers were perfused with Krebs-Henseleit buffer and trace amounts of [1-^{14}C]-octanoate as shown by the horizontal bars. Data are the mean ± standard error of from 4 liver perfusion experiments for each condition. Full symbols (●■▲◆) represent control rats and empty symbols (○□△◇) represent arthritis rats.

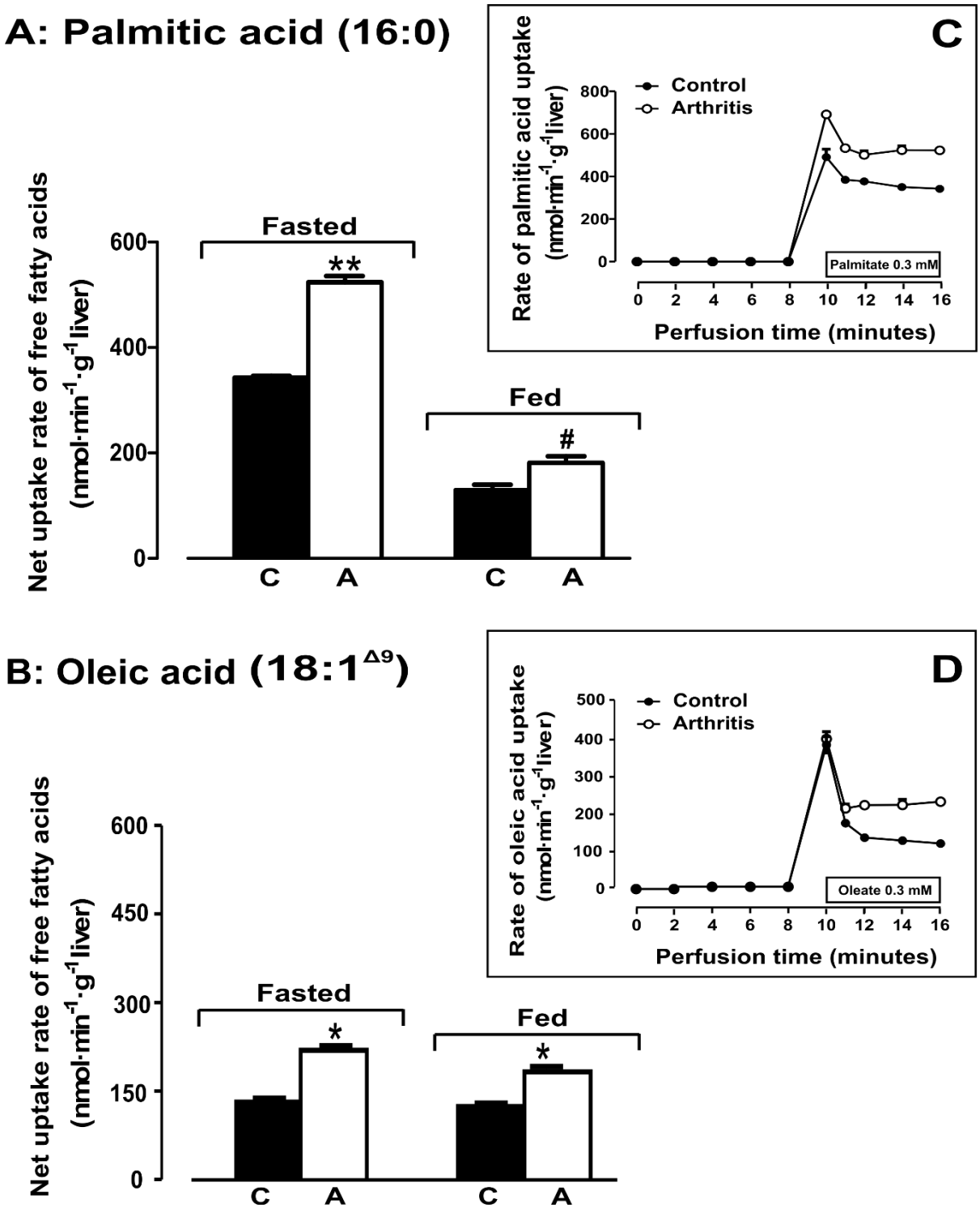

Figure 2: Net uptake rate of free fatty acids (FFA) by perfused livers of control and arthritic rats in the fasted and fed state. Net uptake rate of palmitic acid **(A)** and oleic acid **(B)**. The time courses of palmitic acid and oleic acid uptake shown in the insets (C and D, respectively) were measured in livers from fasted rats. The uptake rates in panels A and B represent steady-state values attained between 12 and 16 minutes perfusion time. Rates were calculated from the portal-venous concentration differences. C, controls and A, arthritis. Data are the mean ± standard error of the mean of 4 perfused livers for each experimental condition. $^{\#}p<0.05$ $^{*}p<0.01$, $^{**}p<0.001$.

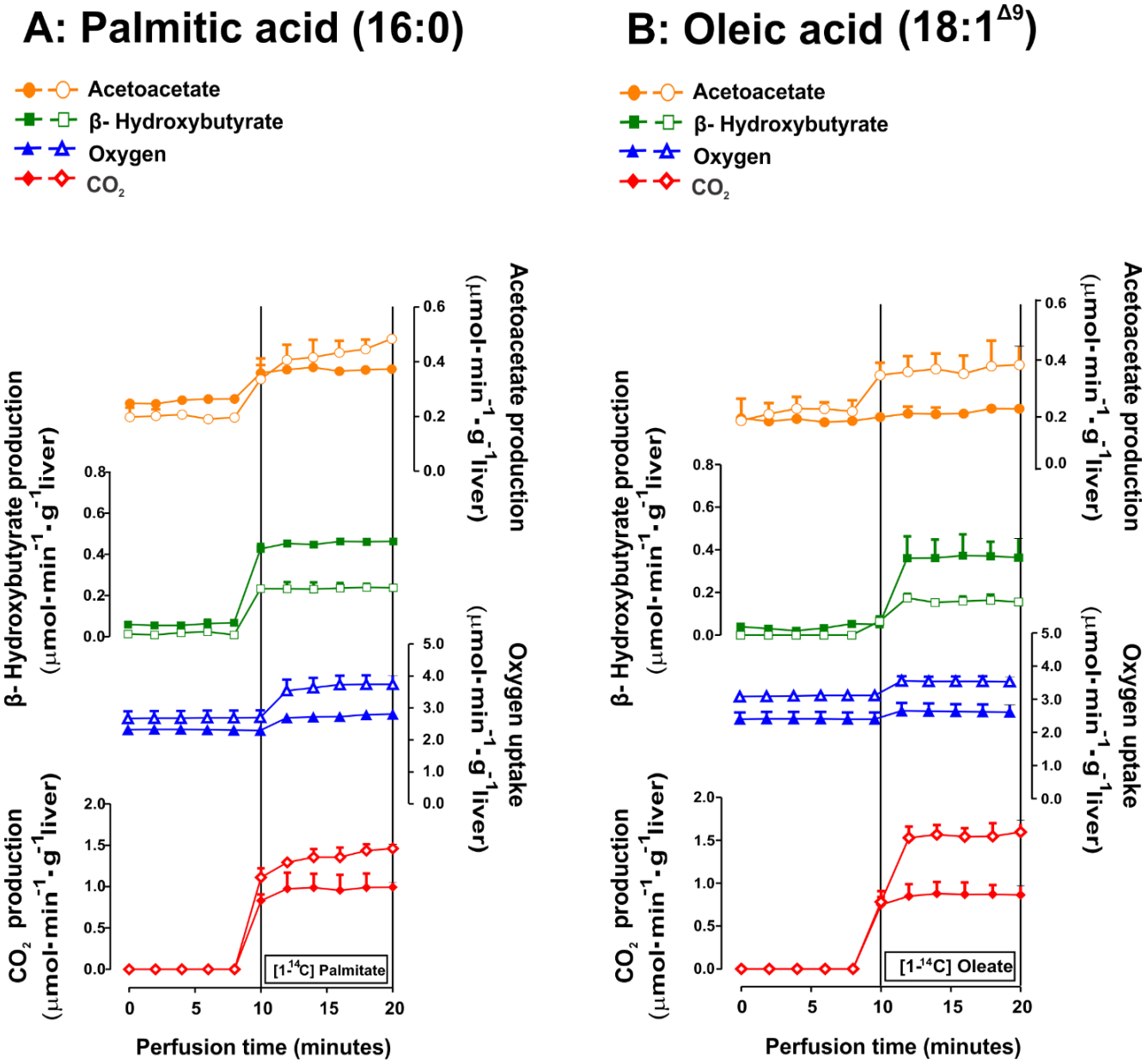

Figure 3: Time course of fatty acids (FA) catabolism in perfused livers of control and arthritic fasted rats. A: Catabolism of palmitic acid. **B**: Catabolism of oleic acid. Livers from 12 h fasted rats were perfused with Krebs/Henseleit-bicarbonate buffer. Palmitic acid (0.3 mM) plus [1-^{14}C]palmitic acid (0.2 µCi·mL^{-1}) or oleic acid (0.3 mM) plus [1-^{14}C]oleic acid (0.2 µCi·mL^{-1}) were infused during 20 minutes (horizontal bars). Data are the mean ± standard error of the mean from 4 liver perfusion experiments for each condition. Full symbols (● ■ ▲ ◆) represent control rats and empty symbols (○ □ △ ◇) represent arthritis rats.

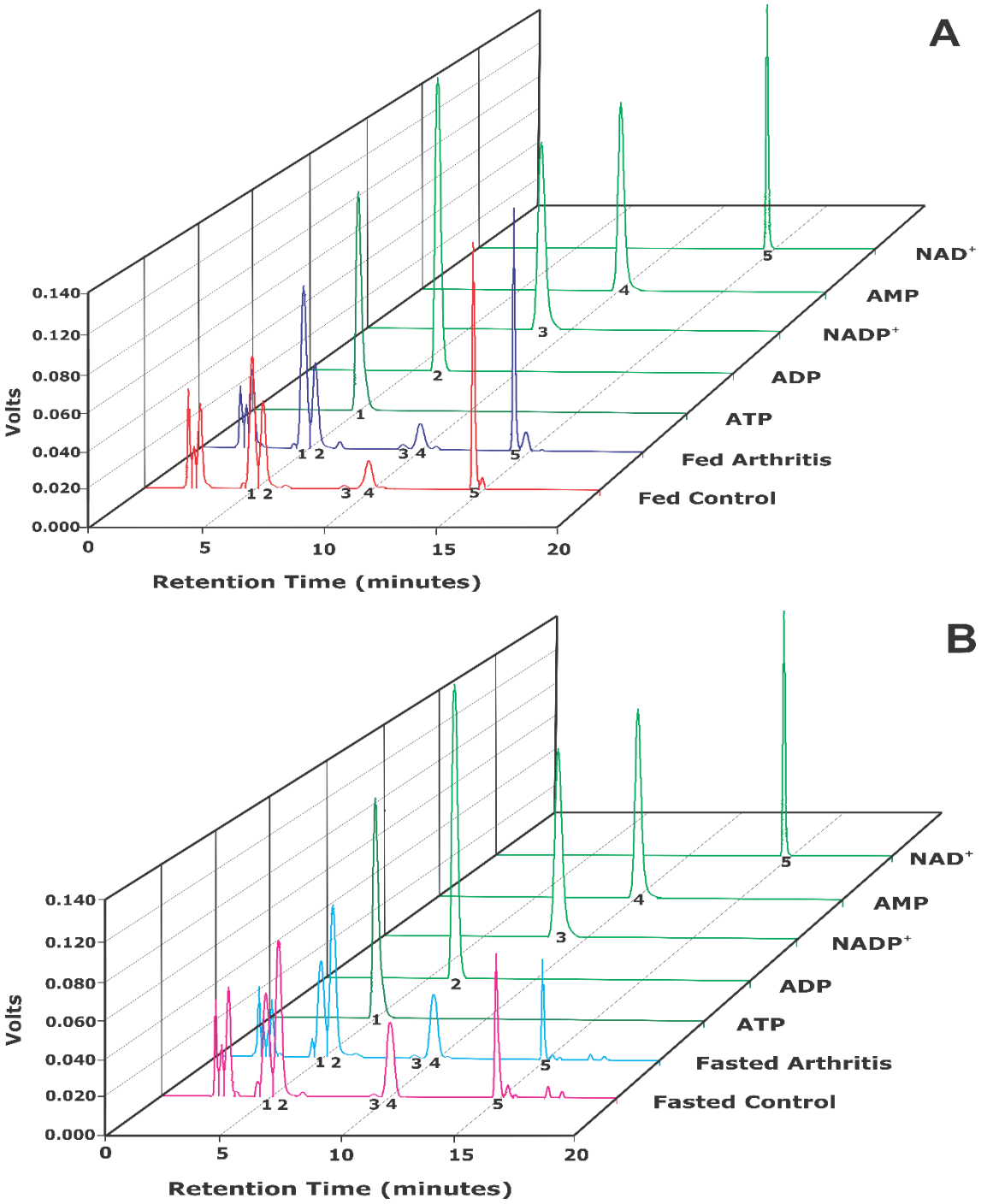

Figure 4: Chromatographic profile of acid-stable adenine nucleotides in the liver of control and arthritic rats. A: Fed state B. Fasted state. Acid-stable nucleotides of freeze-clamped livers were extracted with perchloric acid as described in the Methods section. The samples were separated by HPLC with UV monitoring (254 nm). Peak legends: 1: Adenosine triphosphate (ATP); 2: Adenosine diphosphate (ADP); 3: Nicotinamide adenine dinucleotide phosphate ($NADP^+$); 4: Adenosine monophosphate (AMP) and 5: Nicotinamide adenine dinucleotide (NAD^+). The concentration of the standards was 100 μM and samples were diluted 10 times.

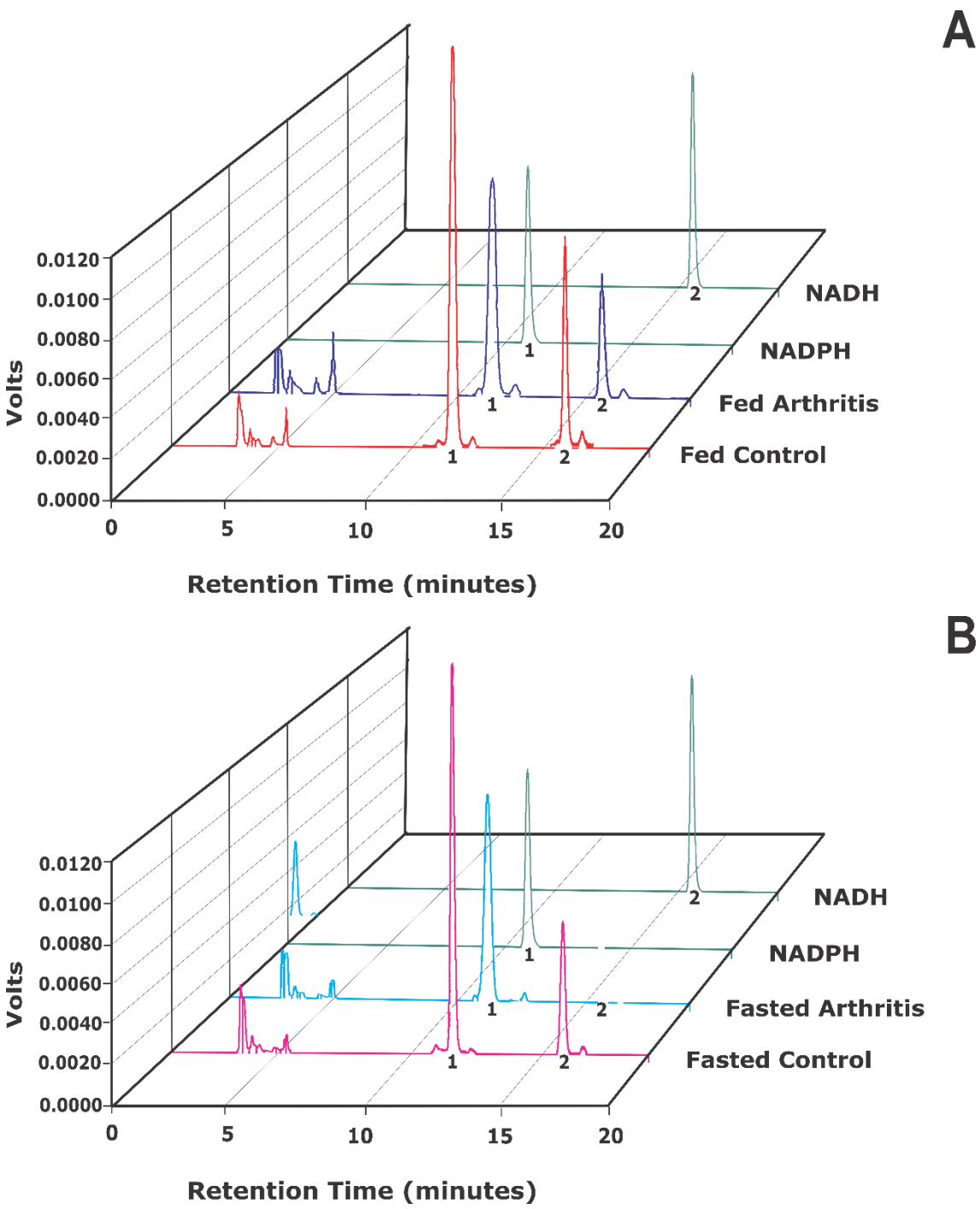

Figure 5: Chromatographic profile of acid-labile adenine nucleotides in the liver of control and arthritic rats. A: Fed state B. Fasted state. Acid-labile nucleotides of freeze-clamped livers were extracted with ethanol and KOH as described in the Methods section. The samples were separated by HPLC with UV monitoring (340 nm). Peak legends: 1: Nicotinamide adenine dinucleotide phosphate reduced form (NADPH) and 2: Nicotinamide adenine dinucleotide reduced form (NADH). The concentration of standards was 100 μM.

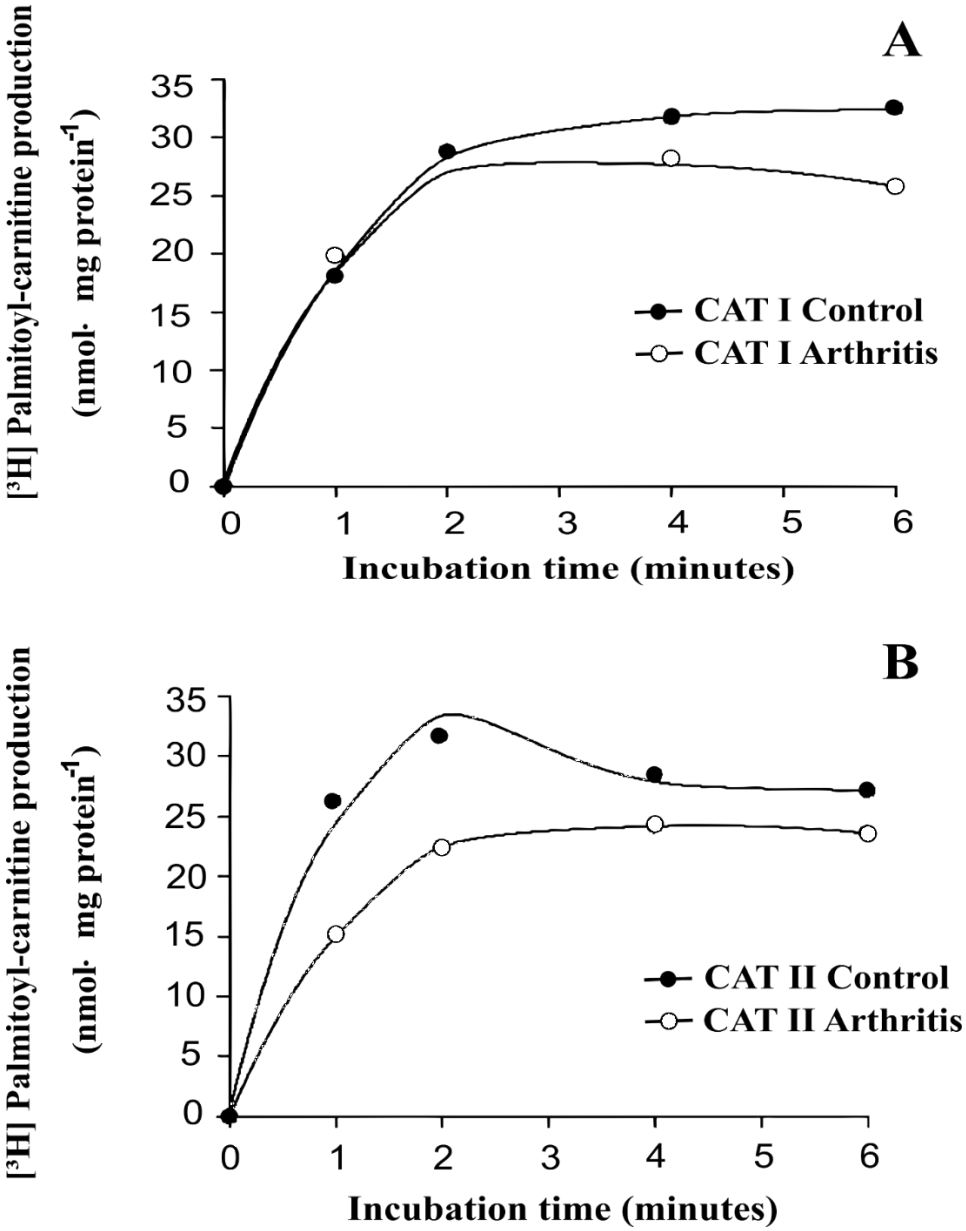

Figure 6. Time courses of [³H]palmitoyl-carnitine formation in the incubation media containing substrates and CAT I (A) and CAT II (B). Fractions containing CAT I and CAT II activities were isolated from hepatic mitochondria from control and arthritic rats as described in the Methods section. The incubation system was: 50 mM manitol, 75 mM KCl, 5% fatty acid-free bovine-serum albumin, 2 mM KCN, 25 mM EGTA, 50 μM palmitoyl-CoA, 0.5 mM carnitine plus 5 μCi/μmol [³H]carnitine and approximately 0.3 mg protein·mL^{-1} of either CAT I or CAT II preparation. The [³H]palmitoyl-carnitine was extracted with butanol. Data are the mean ± standard error of the mean from 4 independent preparations. Each of set data was fitted to a polynomial of the third degree by means of least-square procedure. The continuous lines represent the fitted curves.

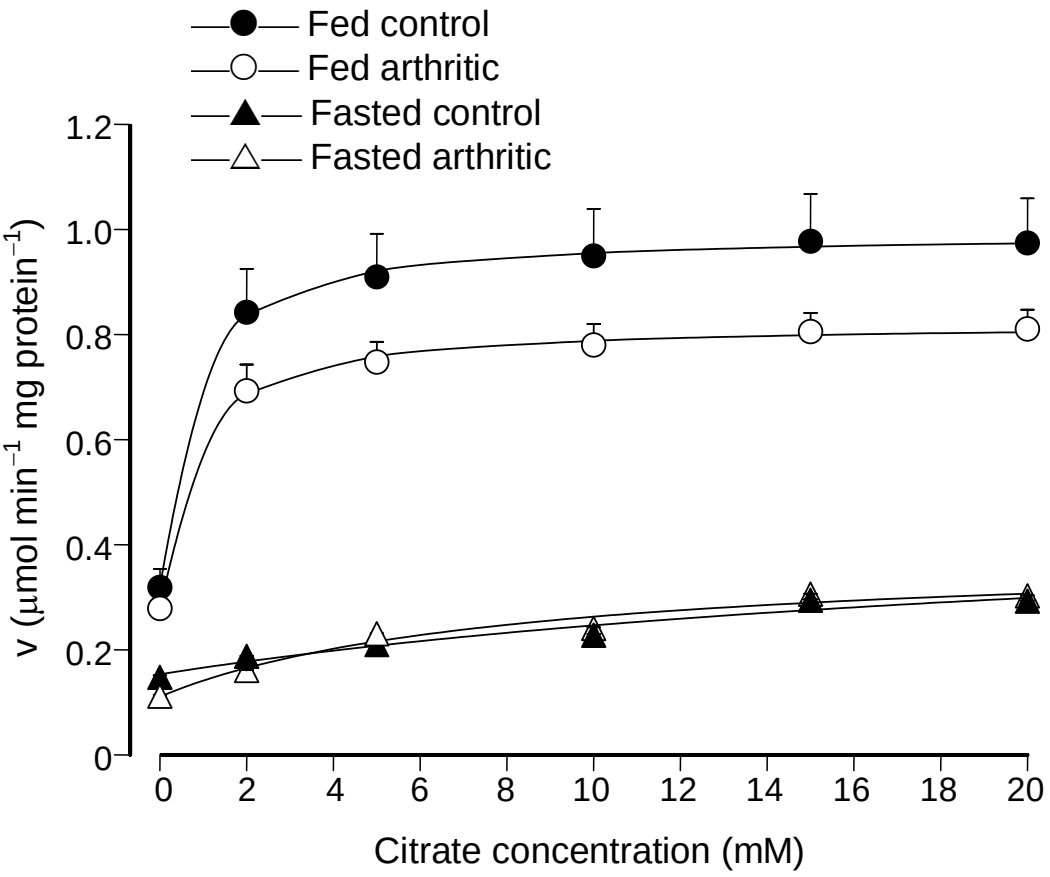

Figure 7. Reaction rate of hepatic acetyl-coenzyme A carboxylase (ACC) from control and arthritic rats in the fed and fasted states as a function of citrate concentration. The enzymatic activity was measured at 37°C as described in Materials and Methods section. The experimental points are the means ± standard error of 4 animals in each experimental condition. The lines were calculated by means of equation (1) with the optimized parameters obtained by fitting the experimental data to the equation. Control/arthritic fed rats: v_o = 0.319±0.010 μmol min^{-1} mg^{-1}/0.278±0.010 μmol min^{-1} mg^{-1} (p = 0.001); V_{max} = 0.673±0.012 μmol min^{-1} mg^{-1}/0.543±0.013 μmol min^{-1} mg^{-1} (p = 0.001); K_{act} =0.602±0.065 mM/0.661±0.087 mM (p = 0.32). Control/arthritic fasted rats: v_o = 0.153±0.015 μmol min^{-1} mg^{-1}/0.111±0.017 μmol min^{-1} mg^{-1} (p = 0.009); V_{max} = 0.329±0.215 μmol min^{-1} mg^{-1}/0.274±0.051 μmol min^{-1} mg^{-1} (p = 0.64); K_{act} =25.40±29.14 mM/8.06±4.47 mM (p = 0.58). The error parameters are standard deviations of the estimate and the p values were obtained by applying Student's t test to each pair or data.

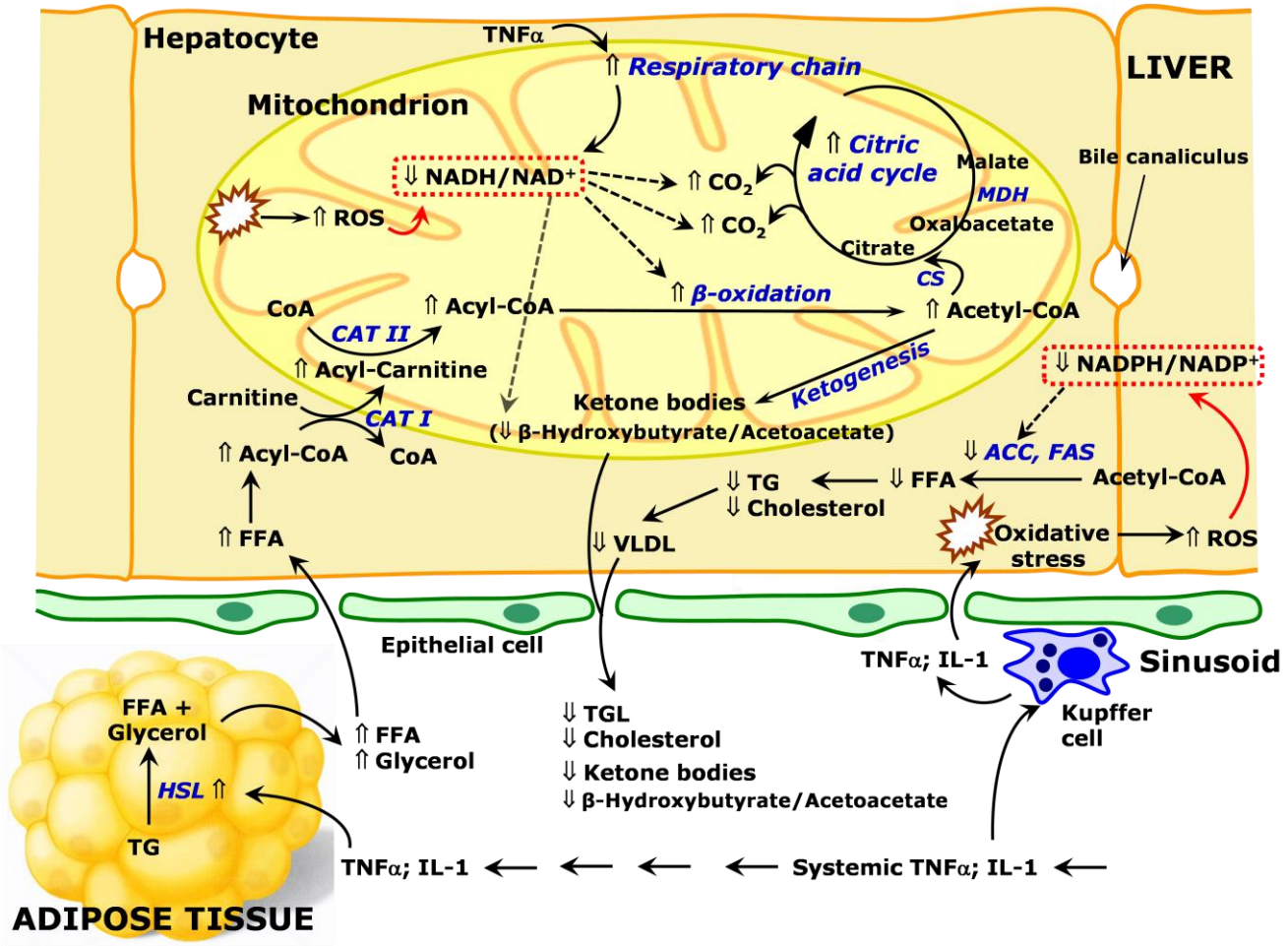

Figure 8. Schematic representation of integrated lipid metabolism occurring in the adipose tissue and liver of arthritic rats with severe cachexia. The scheme is discussed in the text and is based on the results of the current work and on previously published data. The symbol ⇑ means up-regulation and ⇓ down-regulation. Red arrows indicate effects of oxidative stress. Abbreviations: TNF-α, tumor necrosis factor alpha; IL-1, interleukin 1; FFA, free fat acids; TG, triglycerides; VLDL, very low density lipoprotein; HSL, hormone sensible lipase; FAS, fatty acid synthase; ACC, acetyl-CoA carboxylase; MDH, malate dehydrogenase; CS, citrate synthase; CAT I and II, carnitine acyltransferase I and II; CoA, coenzyme A; ROS, reactive oxygen species.

The pentose phosphate pathway is stimulated in the liver of arthritic rats

Mariana M. N. Wendt[1], Ângela V. Parizotto[1], Ciomar A. Bersani-Amado[2], Adelar Bracht[1], Jurandir F. Comar[1*]

[1] Department of Biochemistry, State University of Maringa, PR, Brazil

[2] Department of Pharmacology and Therapeutics, State University of Maringa, PR, Brazil

Address for correspondence:

*Jurandir Fernando Comar

Department of Biochemistry

University of Maringá

87020900 Maringá, Brazil

Email: jurandircomar@yahoo.com.br

Running head: Pentose phosphate pathway in the arthritic liver

Total number of text figures and tables: 4

Grant sponsor: Conselho Nacional de Desenvolvimento Científico e Tecnológico (CNPq); Grant number: 447876/2014-7

ABSTRACT

The oxidative stress is greatly increased in the liver of rats with adjuvant-induced arthritis, a model for rheumatoid arthritis. The ratios of reduced to oxidized glutathione (GSH/GSSG) and NADPH to $NADP^+$ are decreased in the liver of these animals and have been reported to intensify the oxidative stress in the organ. The cytosolic pentose phosphate pathway (PPP) is the major via to regenerate NADPH from $NADP^+$ in the liver cells and, therefore, the present study aimed to estimate the flux of glucose through the PPP in the liver of Holtzman rats with adjuvant-induced arthritis. The latter should allow extrapolations for patients with rheumatoid arthritis. The difference in the rate of $^{14}CO_2$ release from labelled [6-^{14}C]glucose and [1-^{14}C]glucose in the perfused livers was calculated to estimate the fraction of glucose that is metabolized through PPP. The hepatic content of adenine dinucleotides and glutathione was additionally assessed in the liver to evaluate the redox status. The flux of glucose through the PPP was 60% higher in the liver of arthritic rats (compared to the controls). The NADPH/$NADP^+$ and GSH/GSSG ratios were, respectively, 32 and 45% lower in the arthritic liver. The hepatic levels of total dinucleotides phosphate (NADPH + $NADP^+$) and total glutathione were strongly reduced in arthritic rats (40%). The activities of glucose 6-phosphate dehydrogenase and transaldolase were increased in the livers of fasted arthritic rats. The content of glucose 6-phosphate was 25% higher in the arthritic liver and it shows that the rate of glucose phosphorylation is not limiting the flux through PPP. On the contrary, the decreased NADPH/$NADP^+$ ratio is possibly stimulating the flux of glucose through PPP and, by extension, the NADPH regeneration in the liver of arthritic rats. These results reveal that the accentuated oxidative stress in the liver of arthritic rats exceeds the rate of NADPH regeneration in the PPP and this phenomenon is possibly the consequence of the reduced hepatic content of total adenine dinucleotides phosphate and glutathione.

Key words*: adjuvant-induced arthritis, rheumatoid arthritis, hepatic oxidative stress, pentose phosphate pathway, perfused rat liver.*

Abbreviations: PPP, pentose phosphate pathway; G6PDH, glucose 6-phosphate dehydrogenase; ROS, reactive oxygen species; GSH, reduced glutathione; GSSG, oxidized glutathione; TNF-α, tumoral necrosis factor alpha; IL-1 and 6, interleukin 1 and 6; HPLC, high-performance liquid chromatography; Nfr2, nuclear factor erythroid 2-related 2.

INTRODUCTION

Rheumatoid arthritis is an autoimmune and chronic inflammatory disease that affects primarily the joints and occurs in 0.5-1.0% of the adult population worldwide [Uhlig et al., 2014]. The pathophysiology of arthritis involves an intense cytokine-mediated hyperplasia of the synovial membrane and cartilage and overproduction of reactive oxygen species (ROS), which act as mediators of tissue injury [Misko et al., 2013; Kitas & Gabriel, 2011]. Rheumatoid arthritis is a systemic disease and in addition to the joints other organs are affected, such as brain, heart and lungs [Mcinnes & Schett, 2011]. Oxidative stress is also increased in joints and blood of patients with rheumatoid arthritis [Stamp et al., 2012; Lemarechal et al., 2006].

Metabolic alterations are also prominent in rheumatoid arthritis, as the muscle wasting condition known as rheumatoid cachexia [Roubenoff, 2009]. Metabolic modifications are equally significant in the liver of arthritic rats, which present an accelerated oxidative metabolism, increased fatty acids oxidation, increased glycolysis and reduced gluconeogenesis [Wendt et al., 2018; Sá-Nakanishi et al., 2018; Fedatto et al., 2000; Fedatto et al., 1999]. This indicates that the hepatic metabolism in arthritis seems to be in line with that in the muscle and adipose tissue, i.e., a prevalence of catabolic on anabolic pathways. In addition, oxidative stress is altered in the plasma, liver, brain and heart of arthritic rats [Bracht et al., 2016; Schubert et al., 2016; Wendt et al., 2015; Comar et al., 2013]. Particularly in the arthritic liver, where metabolic alterations and inflammation are prominent, the oxidative stress is quite pronounced when compared to other organs [Wendt et al., 2015; Comar et al., 2013].

The levels of ROS, protein carbonyl groups and lipoperoxides are increased in the liver of arthritic rats, particularly in the mitochondria, peroxisomes and cytosol of hepatic cells [Comar et al., 2013]. The reduced glutationa (GSH) was strongly diminished and the oxidized glutathione (GSSG) increased in all these cellular compartments of the arthritic liver. The cytokine-induced stimulation of the pro-oxidant system has been reported to contribute increasing the oxidative stress in the liver of arthritic rats, but a deficient antioxidant defence, specifically the lower GSH/GSSG ratio, seems to be critical to modify the oxidative state in the organ [Comar et al., 2013]. The activity of glutathione peroxidase and reductase are not limiting, respectively, the oxidation and regeneration of GSH in

the arthritic liver [Comar et al., 2013]. Thus, the critical point seems to be the hepatic content of NADPH, which is the electron donor substrate to regenerate GSH from GSSG. Indeed, the ratio of NADPH/$NADP^+$ is decreased in the liver of arthritic rats [Wendt et al., 2018]. The cytosolic pentose monophosphate pathway is the major cellular via to regenerate NADPH from $NADP^+$ and it is normally stimulated in tissues that are under increased oxidative stress [Stincone et al., 2015]. Thus, it is possible that the activity of this pathway may limit the rate of NADPH regeneration in the liver of arthritic rats.

The rate of NADPH regeneration in the pentose phosphate pathway (PPP) is additionally increased in tissues that present an elevated synthetic rate, such as liver [Stincone et al., 2015]. Thus, the flux of glucose through PPP may modulate the synthesis of biomolecules in the liver, such as lipids, by means of modifications in the levels of cytosolic NADPH. In rheumatoid cachexia, the whole-body protein breakdown is stimulated and, particularly in the severe rheumatoid cachexia, the adipose tissue lipolysis is additionally increased and associated with reduced body weight and increased rate of mortality [von Haehling & Anker, 2014; Summers et al., 2010]. Indeed, the synthesis of fatty acids seems to be diminished in the arthritic liver due to reduced levels of NADPH in the cytosol [Wendt et al., 2018]. Such a condition should be contributing not only to increase the oxidative stress in the liver but also to the marked cachexia that occurs in rats with adjuvant-induced arthritis and possibly in patients with severe rheumatoid arthritis.

The PPP is divided into oxidative and non-oxidative phases. In the oxidative phase, two moles of $NADP^+$ are converted into two moles of NADPH for each mole of glucose 6-phosphate that is oxidized into one mole of pentose 5-phosphate (+ one mole of CO_2). In the non-oxidative phase of PPP, five moles of glucose 6-phosphate are regenerated from six moles of pentose 5-phosphate. Glucose 6-phosphate dehydrogenase (G6PDH) is the limiting enzyme of the oxidative phase of PPP and transaldolase is the key enzyme of the reversible non-oxidative branch of the PPP [Banki et al., 1996; Eggleston & Krebs, 1974; Novello & Mclean, 1968]. G6PDH is positively modulated by $NADP^+$ and both the activity and expression of the enzyme are increased in the liver of arthritic rats [Comar et al., 2013; Fahim et al., 1995; Yasmineh et al., 1991]. In addition, the activity of G6PDH and transaldolase are increased in the liver of rats with TNFα-induced cachexia [Yasmineh & Theologides, 1992; Yasmineh et al., 1991].

If on the one hand the decreased ratio of NADPH/$NADP^+$ may be attributed to reduced activity of PPP, on the other it should stimulate the activity of PPP in the liver of arthritic rats, especially if is associated with higher activity of G6PDH. In this case, the decreased NADPH/$NADP^+$ ratio would be the result of an accentuated consume of NADPH to improve unsuccessfully the accentuated hepatic oxidative stress. Therefore, the present study aimed to estimate the flux of glucose through the PPP in the liver of Holtzman rats with adjuvant-induced arthritis, which should also allow extrapolations for patients with severe rheumatoid arthritis. The hepatic content of adenine dinucleotides and glutathione was additionally assessed in the liver to evaluate the redox status.

MATERIALS AND METHODS

Materials

The liver perfusion apparatus was built in the workshops of the University of Maringá. Enzymes and coenzymes were purchased from Sigma Chemical Co. (St. Louis, MO, USA). Labeled [1-^{14}C]glucose (56 mCi·mmol^{-1}) and [6-^{14}C]glucose (60 mCi·mmol^{-1}) were purchased from New England Nuclear (Boston, MA, USA). All other chemicals were of analytical grade.

Animals and induction of arthritis

Male *Holtzman* rats weighting 180-210 g (50 days old) were obtained from the Center of Animal Breeding of the State University of Maringá (UEM) and maintained in standard laboratory conditions at a temperature of 24±3ºC under a regulated 12h light/dark cycle. The animals were housed in conventional steel cages (3 rats/cage) and were fed *ad libitum* with a standard laboratory diet (Nuvilab®, Colombo, Brazil). For arthritis induction, animals were injected subcutaneously in the left hind paw with 0.1 ml (500 µg) of Freund's adjuvant (heat inactivated *Mycobacterium tuberculosis*, derived from the human strain H37Rv), suspended in mineral oil [Bracht et al., 2016]. Animals were used for experiments at day 18th after adjuvant injection. Rats of similar ages served as controls. All procedures followed the guidelines of the Brazilian Council for the Control of Animal Experimentation (CONCEA) and were previously approved by the Ethics Committee for Animal Experimentation of the State University of Maringá (Protocol number 094/2013-CEEA).

Liver perfusion

Hemoglobin-free, non-recirculating liver perfusion was performed as previously described [Comar et al., 2003]. Fed rats were deeply anesthetized with sodium thiopental (100 mg·kg^{-1}) plus lidocaine (10 mg·Kg^{-1}). After cannulation of the portal and cava veins, the liver was removed and positioned in a plexiglass chamber. The perfusion fluid was Krebs/Henseleit-bicarbonate buffer (pH 7.4), saturated with a mixture of oxygen and carbon dioxide (95:5) by means of a membrane oxygenator with simultaneous temperature adjustment to 37ºC. The flow was maintained constant by a peristaltic pump (Minipuls 3,

Gilson, France) and it was adjusted to between 30 and 33 $mL \cdot min^{-1}$. Oxygen concentration in the venous perfusate was monitored by a teflon-shielded platinum electrode. Samples of the effluent perfusion fluid were collected at two minutes intervals and analyzed for their metabolite content.

Activity of pentose phosphate pathway (PPP)

The glucose metabolized through the pentose phosphate pathway (PPP) was performed as previously described by Katz & Woods [1963] and reviewed by Larrabe [1990], with some modifications. Livers from fed rats were perfused with Krebs/Henseleit-bicarbonate buffer. After stabilization of the oxygen uptake, the livers were perfused with 10 mM glucose during 30 minutes. Trace amounts of [1-^{14}C]glucose or [6-^{14}C]glucose (0.2 $\mu Ci \cdot mL^{-1}$) were infused simultaneously. The perfusate effluent was collected in Erlenmeyer flasks and carbon dioxide was measured by trapping $^{14}CO_2$ in phenylethylamine [Comar et al., 2010]. Radioactivity was measured by liquid scintillation spectrometry (TriCarb 2810 TR counter, Packard-PerkinElmer) and the results expressed as fraction of the inflowing radioactivity. The following scintillation solution was used: toluene/ethanol (2:1) containing 5 $g \cdot L^{-1}$ 2,5-diphenyloxazole and 0.15 $g \cdot L^{-1}$ 2,2-p-phenylenebis(5-phenyloxazole).

The pathways that release CO_2 from glucose in considerable amounts under these conditions are the citric acid cycle and PPP. The citric acid cycle produces $^{14}CO_2$ from both [1-^{14}C]glucose and [6-^{14}C] glucose, but PPP produces $^{14}CO_2$ only from [1-^{14}C]glucose. As [1-^{14}C]glucose and [6-^{14}C]glucose are infused into different livers it is possible to calculate the fraction of glucose uptake that was metabolized through PPP using the following expression:

$$\frac{3 \cdot F_{met}}{(1 + 2 \cdot F_{met})} = \frac{([1]CO_2 / G) - ([6]CO_2 / G)}{1 - ([6]CO_2 / G)} \qquad \text{Eq. (1)}$$

In Eq. (1) F_{met} is the fraction of glucose uptake that was metabolized by PPP, G is the rate of glucose uptake by the liver, $[1]CO_2$ and $[6]CO_2$ is the rate of $^{14}CO_2$ release from [1-^{14}C]glucose and [6-^{14}C]glucose, respectively.

Liver freeze clamped for homogenate preparation

Two protocols were used to prepare the liver homogenate: 1) the peritoneal cavity from fed and fasted anesthetized rats were surgically exposed, the liver was removed, freeze-clamped and stored in liquid nitrogen to assess the enzyme activities and the hepatic content of glutathione and glucose 6-phosphate; and 2) the livers were removed from the perfusion apparatus in the end of perfusion period (stead-state; at 40 minutes in Figure 1) and freeze-clamped in liquid nitrogen to assess the hepatic content of glycogen and adenine dinucleotides. The homogenate preparation was separately descried below for each specific parameter.

Hepatic content of glycogen

The hepatic content of glycogen was determined enzymatically after freeze-clamping the perfused livers [Bergmeyer, 1974]. Portions of approximately 2 g of tissue were extracted with 10 mL of 0.6 M perchloric acid. Glycogen in the extract was hydrolysed using amyloglucosidase. The reaction mixture contained 0.1 M potassium hydrogen carbonate, 0.135 M acetate buffer (pH 4.8) and 0.75 units of amyloglucosidase. After 2 hours incubation at 40° C the reaction was stopped by adding of 0.6 M perchloric acid. The mixture was centrifuged and neutralized with potassium hydrogen carbonate and free glucose was determined with a commercial kit. The results were expressed as μmol glucosyl units per gram liver.

Hepatic content of adenine dinucleotides

For measuring of the acid-stable adenine nucleotides ($NADP^+$ and NAD^+), the liver was freeze-clamped after perfusion and 2 g were macerated in liquid nitrogen and three volumes of 0.6 M perchloric acid were added to the powder tissue. The suspension was then homogenized in a van Potter-Elvehjem homogenizer and the resulting homogenate centrifuged at 4,000*g* for 10 minutes. The supernatant was neutralized with potassium carbonate, filtrated and used for nucleotides determination by high-performance liquid chromatography (HPLC) analysis.

The acid-labile NADH and NADPH were extracted as previously described [Kalhorn et al., 1985] with some modifications. Briefly, 1.5 g of freeze-clamped

liver was macerated in liquid nitrogen and 10 mL of ethanol was added to the powder tissue. The suspension was homogenized and 2 mL was transferred to a solution containing ethanol and 5 M KOH (99:1%). After centrifugation at 2500*g* for 5 minutes, the pellet was suspended in 1 mL of ethanol plus 2 mL of chloroform and centrifuged at 14,000*g* for 5 minutes. The aqueous phase was neutralized with 0.1 M phosphate buffer (pH 7) and centrifuged at 12,000*g* for 3 minutes. The supernatant was filtered and used for nucleotide determinations by HPLC analysis.

The HPLC system (Shimadzu, Japan) consisted of a system controller (SCL-10AVP), two pumps (model LC10ADVP), a column oven (model CTO-10AVP) and an UV– Vis detector (model SPD-10AV). A reversed-phase C18 CLC-ODS column (5 µm, 250 × 4.6 mm i.d.; Shimadzu) protected with a CLC-ODS precolumn (5 µm, 4 × 3 mm i.d.; Phenomenex), was used with a gradient from reversed-phase 0.044 $M \cdot L^{-1}$ phosphate buffer solution (pH 6.0) to 0.044 $M \cdot L^{-1}$ phosphate buffer solution plus methanol (1:1; pH 7.0). For acid-stable nucleotides, in percent methanol, the gradient was the following: at 0 min, 0%; at 2.5 min, 0.5%; at 5 min, 3%; at 7 min, 5%; at 8 min, 12%; at 10 min, 15%; at 12 min, 20%; at 20 min, 30%. For NADH and NADPH, the gradient was linear from 0-20 minutes ranging from 0 to 30% of methanol. The temperature was kept at 35 °C and the injection volume was 20 µL with a flow rate of 0.8 $mL \cdot min^{-1}$. Monitoring was performed spectrophotometrically at 254 nm for acid-stable nucleotides and at 340 nm for NADH and NADPH.

Identification of the peaks of investigated compounds was carried out by a comparison of their retention times with those obtained by injecting standards under the same conditions. The concentrations of the compounds were calculated by means of the regression parameters obtained from the calibration curves. The calibration curves were constructed by separating chromatographically standard solutions of the compounds. Linear relationships were obtained between the concentrations and the areas under the elution curves.

Glutathione content

The liver content of reduced (GSH) and oxidized (GSSG) glutathione were extracted as previously described [Begic et al., 2016]. Briefly, 1.0 g of freeze-clamped liver was macerated in liquid nitrogen and 5mL of cold 0.9% sodium

chloride were added to the powder tissue. The suspension was then homogenized in a van Potter-Elvehjem homogenizer and 1 mL was transferred to a solution containing 5% metaphosphoric acid (MPA). After centrifugation at 7600*g* for 20 minutes, the supernatant was filtered and used for GSH and GSSG quantification by HPLC analysis. For the identification of the peaks, a 20 minutes isocratic run of 0.1 $M \cdot L^{-1}$ $NaClO_4$ plus 1% H_3P0_4 (pH 3.0) was used. The temperature was kept at 40°C and the injection volume was 20 µL with a flow rate of 1 $mL \cdot min^{-1}$. Monitoring was performed spectrophotometrically at 215 nm.

Hepatic levels of glucose 6-phosphate

The hepatic content of glucose 6-phosphate was determined by an enzymatic procedure using yeast glucose 6-phosphate dehydrogenase [Bergmeyer, 1974]. Briefly, 2.0 g of freeze-clamped liver were macerated in liquid nitrogen and two volumes of 2 M perchloric acid were added to the powder tissue. The suspension was then homogenized in a van Potter-Elvehjem homogenizer and the resulting homogenate centrifuged at 4,000*g* for 10 minutes. The supernatant was neutralized with 5 M potassium carbonate. After precipitation of the potassium perchlorate, the supernatant, with pH between seven and eight, was used for the assay. The assay system contained 2 mM $NADP^+$, 5 mM $MgCl_2$, 50 mM Tris (pH 7.6) and glucose 6-phosphate dehydrogenase (1.9 $U \cdot mL^{-1}$).

Glucose-6-phosphate dehydrogenase (G6PDH) and transaldolase assay

For the determination of the G6PDH and transaldolase activities, 1 g of freeze-clamped liver were macerated in liquid nitrogen, homogenized in a van Potter-Elvehjem homogenizer with ten volumes of 0.1 M phosphate buffer (pH 7.4) and centrifuged at 20.000*g* for 30 minutes. The supernatant was used to measure the enzyme activities by spectrophotometry.

The activity of G6PDH was assayed by increasing the absorbance at 340 nm due to NADPH formation dependent on the consumption of glucose-6-phosphate [Bergmeyer, 1974]. The activity of transaldolase was determined at 340 nm by the oxidation of NADH in the presence of fructose 6-phosphate, erythrose 4-phosphate and the enzyme glyceraldehyde 3-phosphate dehydrogenase [Bergmeyer, 1974].

Statistical analysis

The error parameters presented in graphs and tables are standard errors of the means. Statistical analysis was done by means of the GraphPad Prism Software (version 5.0). The Student's t test was applied and the 5% level ($p < 0.05$) was adopted as a criterion of significance. Numerical analysis (initial rates of glucose 6-phosphate dehydrogenase) was done by means of the Scientist® program from MicroMath Scientific Software.

RESULTS

Activity of pentose phosphate pathway (PPP)

Figure 1 illustrates the time courses of [1-^{14}C]glucose and [6-^{14}C]glucose infusion and $^{14}CO_2$ release and oxygen consumption in the liver of fed rats. In order to compare the groups, the numerical values of CO_2 release at 40 minutes perfusion time in Figure 1 (steady-state) were displayed in Table I. CO_2 release from [1-^{14}C]glucose and [6-^{14}C]glucose was 24% and 36% higher, respectively, in the livers of arthritic rats, but oxygen consumption was not different. The glucose uptake (G) was 25% lower in the arthritic livers. The fraction of uptake glucose that was metabolized through the PPP (F_{met}) was calculated using Eq. (1) and it was 60% higher in the livers of arthritic rats.

Hepatic content of glycogen and adenine dinucleotides

The effects of 10 mM glucose infusion on the levels of glycogen, NAD^+, $NADP^+$, NADH and NADPH were measured in the liver of fed control and arthritic rats. For this purpose, the livers were freeze-clamped in liquid nitrogen at 40 minutes perfusion time in Figure 1. The results are shown in Table I. Glycogen content in arthritic livers were only one quarter of that found in the control liver. Hepatic levels of $NADP^+$ and NAD^+ were 15 and 14% lower in the liver of arthritic rats. The hepatic levels of NADPH were 52% lower in arthritic rats, but the levels of NADH were not different. The NADPH/$NADP^+$ and NADH/NAD^+ ratios were, respectively, 32 and 19% lower in the arthritic livers.

Enzyme activities

Considering that glucose flux through PPP was increased in the liver of arthritic rats and considering that the major regulatory point of PPP is the first reaction catalyzed by G6PDH, the activity of this enzyme was measured in the liver homogenate from fasted and fed rats. Figure 2 shows the reaction rates (v) as a function of glucose 6-phosphate concentration, which were analyzed in terms of Michaelis-Menten equation: $v = V_{max} \cdot [G6P]/(K_M + [G6P])$, where [G6P] is the concentration of glycose 6-phosphate. The maximal reaction rates (V_{max}) and the Michaelis–Menten constants (K_M) were computed by fitting this equation to

the experimental data using a nonlinear iterative least-squares procedure. The points (v) in Figure 2 are the experimental data (mean ± SEM) and the continuous lines represent the theoretical curves that were calculated with the Michaelis-Menten equation using the kinetic parameters given in the legend. Analysis of the V_{max} and K_M values reveals that only V_{max} in fasted rats was higher (+95%) in the arthritic state. The experimental values of G6PDH activity measured with excess of substrate are shown in the lower part of Table 2, which also shows the transaldolase activity. As expected the G6PDH activity was higher (+93%) in arthritic livers from fasted rats. The activity of transaldolase, a key enzyme of the reversible non-oxidative phase of PPP, was 55% higher in the liver of fasted arthritic rats, but not different in the fed state.

Hepatic levels of glutathione and glucose 6-phosphate

The levels of GSH, GSSG and glucose 6-phosphate were measured in the liver of control and arthritic rats in the fed and fasted state. Table II shows the values of these parameters in $nmol \cdot g^{-1}$ of liver. The levels of glucose 6-phosphate were 21 and 29%, respectively, in the liver of fasted and fed arthritic rats. The levels of GSH were 19 and 36% lower, respectively, in the liver of fasted and fed arthritic rats. The levels of GSSG were 48% higher in the livers of arthritic rats but only in the fasted state. The content of total glutathione (GSH + 2xGSSG) was 35% and 20% lower, respectively in the livers of fed and fasted arthritic rats. The GSH/GSSG ratios were 45 and 30% lower, respectively, in fasted and fed arthritic rats.

DISCUSSION

The experimental model of chronic inflammation used in the present study is considered a model of severe arthritis in rats and it shares features of advanced and uncontrolled rheumatoid arthritis [Stolina et al., 2009; Hegen et al., 2008]. These animals present a generalized inflammatory manifestations and severe cachexia that resembles that occurring in chronic wasting diseases, in which muscle wasting is associated with adipose wasting and reduced body weight [Bracht et al., 2016; Hegen et al., 2008]. Before discussing the results obtained in the present study in detail it seems worth to summarize the most important findings. In the livers of arthritic rats (1) the flux of glucose through pentose phosphate pathway (PPP) is increased; (2) the NADPH/$NADP^+$ and NADH/NAD^+ ratios are decreased; (3) the glycogen content is decreased; (4) the levels of glucose 6-phosphate are increased; (5) the levels of GSH and GSH/GSSG ratio are reduced; (6) the levels of total adenine dinucleotides (NADPH + $NADP^+$) and glutathione (GSH + 2GSSG) are decreased; and (7) the activity of G6PDH and TAL are increased, but only in fasted state. These results will be discussed in the following paragraphs.

The higher rate of glucose phosphorylation certainly provides glucose 6-phosphate sufficient to maintain an increased flux of glucose through PPP in the liver of arthritic rats. The hepatic levels of $NADP^+$, the other limiting substrate of PPP, were decreased in arthritic rats. However, the hepatic levels of NADPH, which modulates negatively the enzyme G6PDH and by extension the PPP, were strongly reduced in arthritic rats. Therefore, the resulting ratio of NADPH/$NADP^+$ is reduced and it is possibly stimulating the activity of PPP in the arthritic livers. Although the hepatic levels of $NADP^+$ were lower in arthritic rats (compared to the controls), the lower NADPH/$NADP^+$ ratio shows that the oxidized form of NADP is available to NADPH regeneration. Thus, if PPP is stimulated and both glucose 6-phosphate and $NADP^+$ are available, the rate of NADPH regeneration is not restricted in the liver of arthritic rats. The same occurs with the GSH regeneration, i.e., the activity of glutathione reductase is not modified and one of the substrates of this enzyme, GSSG, is not decreased in the arthritic liver. [Comar et al., 2013]. Thus, only the other substrate, NADPH, should be limiting the GSH regeneration whether it is decreased, as it was. Therefore, the

pronounced oxidative stress in the liver of arthritic rats should be not improved only if the production of reactive species exceeds the NADPH regeneration in the PPP or if the regenerated NADPH is been shunted to other cytosolic NADPH-utilizing processes. This conclusion is allowed because the oxidative stress was increased in the cytosol of hepatocytes of arthritic rats, i.e., in the same cellular compartment where NADPH is been regenerated via PPP [Comar et al., 2013]. In addition to the increased oxidative stress the NADH-dependent oxidative metabolism is accelerated in the arthritic livers and the NADPH might be shunted to NADH-NAD^+ couple via the equilibrium transhydrogenase reaction [Wendt et al., 2018]. The latter is favored if the NADH-NAD^+ couple is shifted toward an oxidized state. The ratio of NADH to NAD^+ was indeed diminished in the arthritic liver, but it reflects the ratio in the total tissue with strong contribution of the mitochondrial ratio [Wendt et al., 2018]. On the contrary, the higher lactate/pyruvate ratio verified in the liver of fed arthritic rats indicates a higher cytosolic NADH/NAD^+ ratio, a condition that do not favor the transhydrogenase reaction [Wendt et al., 2018; Castro-Ghizoni et al., 2017; Fedato et al., 2000].

It is possible, therefore, that the reactive species production is exceeding the GSH regeneration in the liver of arthritic rats that in turn is decreased due to reduced levels of NADPH. In this regard, the levels of total dinucleotides phosphate (NADPH + $NADP^+$) in the arthritic liver were 42% lower when compared to the controls. The same may be said about the total glutathione (GSH + 2GSSG), which was reduced in the arthritic livers [Sá-Nakanishi et al., 2018; Comar et al., 2013]. Thus, the pronounced oxidative stress in the liver is occurring because the total redox equivalents used to neutralize reactive species are decreased and not because of a deficient interconversion of oxidized into reduced equivalents. In this regard, the cellular redox homeostasis is regulated mainly by nuclear factor erythroid 2-related 2 (Nfr2), a redox-sensible transcription factor which upregulates antioxidant defense genes, particularly enzymes required for NADP and glutathione synthesis [Dinkova-Kostova et al., 2015]. Although Nfr2 activity is unknown in the arthritic liver, it has been reported to be strongly downregulated in chronic and autoimmune inflammatory disorders [Kim et al., 2010]. In addition, Nfr2 is negatively regulated by microRNA 155 (miR-155), which is elevated in synovial fibroblasts from rheumatoid arthritis patients and possibly in the liver of arthritic rats [Guo et al., 2015; Sonkoly & Pivarcsi, 2009]. The diminished activity of Nfr2 in the arthritic

liver might additionally diminish the NADPH regeneration can occur via mitochondrial isocitrate dehydrogenase 1 and cytosolic $NADP^+$-dependent malic enzyme, which are both upregulated by Nfr2 [Dinkova-Kostova et al., 2015]. The latter may be intensifying the oxidative stress verified in the mitochondria of arthritic liver [Comar et al., 2013].

Despite of an increased activity of PPP in the liver of arthritic rats the hepatic glucose uptake was decreased in these animals (-26%; Table I) and this point deserves a few comments. The rate of glucose uptake in the liver of arthritic rats was at the same extension (0.47 $\mu mol \cdot min^{-1} \cdot g^{-1}$) of that metabolized through the glycolysis in perfused livers from fed arthritic rats in the absence of exogenous substrates, i.e., only the glucose derived from liver glycogen [Wendt et al., 2018]. The ratio of control to arthritic glycogen content in non-perfused livers was equal to 1.47 [Fedatto et al., 2001] and this ratio in the present study at the end of perfusion time was 4.07 (Table I). These results show that apparently the hepatic glycogen of arthritic rats was depleted in a higher extension when compared to the control values even under 10 mM glucose infusion, a condition that should save the glycogen content. However, glycogenolysis and glycolysis are increased in the liver of arthritic rats so that the glycogen-derived glucose is metabolized through the glycolysis and maybe in the lower extension metabolized through other pathways [Fedatto et al., 2000]. This because the hepatic efflux of glycogen-derived glucose should be negligible considering the infusion of 10 mM glucose in the perfused livers. Thus, the glucose uptake is reduced in the arthritic liver possibly because of the glycogen-derived glucose. Furthermore, if the latter occurs then the labelled infused glucose is certainly diluted by the glycogen-derived glucose and the flux of glucose through PPP in the arthritic liver verified in the present study is been underestimated.

The activity of transaldolase was not modified in the livers of arthritic rats in the fed state. However, irrespective of being control or arthritic rats, the transaldolase activity was lower in the fasted when compared to the fed state. The latter phenomenon has been reported not only for transaldolase but also for other enzymes of the non-oxidative phase of PPP and it was associated to a reduced plasmatic insulin in fasting [Heinrich et al., 1976]. On the other hand, both G6PDH and transaldolase were increased in the liver of arthritic rats in the fasted state and may be associated with even greater stimulation of PPP in this

nutritional status. However, the flux of glucose through PPP was not estimated in the fasted state and future approach may clarify this point.

The model used to estimate the activity of PPP in the present study presents some limitations. The Eq. (1) is valid only if some assumptions implicit in its use are considered [Larrabe, 1990]. The most of conditions under which the Eq. (1) is applicable are included in the present study, except to be unreliable for non-homogeneous tissue, such as liver, and that the synthesis and degradation of glycogen must be negligible. The first assumption is minimized because the heterogeneity of the liver metabolism is applicable equally to both arthritic and control rats. However, the second assumption is possibly adding some error to estimate the real activity of PPP. As above described the glycogen degradation is increased in liver of arthritic rats, a condition that dilutes the labelled glucose and underestimates the real flux through PPP. One possible solution would be estimate the variation of glycogen content during the infusion of 10 mM glucose, what would permit to calculate the activity of PPP with more precision, but it was not performed in the present study. Anyway, the flux of glucose through PPP in the arthritic liver is increased or further increased if the rate of glycogen catabolism is considered.

Concluding remarks

The results of the present study reveal that the flow of glucose through the pentose phosphate pathway (PPP) is increased in the liver of arthritic rats. The rate of glucose phosphorylation is not limiting the flux through PPP, on the contrary, the decreased NADPH/$NADP^+$ ratio is possibly stimulating the flux of glucose through PPP and, by extension, the rate of NADPH regeneration in the liver of arthritic rats. These results in addition reveal that the accentuated oxidative stress in the liver of arthritic rats exceeds the rate of NADPH regeneration in the PPP and this phenomenon is possibly the consequence of the reduced hepatic content of total adenine dinucleotides phosphate and glutathione.

Acknowledgements

Authors wish to thank the financial support of the Coordenação de Aperfeiçoamento de Pessoal de Nível Superior (CAPES) and of the Conselho Nacional de Desenvolvimento Científico e Tecnológico (CNPq).

Competing interests

The authors declare that no competing interest exists and that all approved the final manuscript.

Authors' contributions

JFC conceived and designed the experiments. CABA induced the arthritis. MMNW and AVP performed the experiments. JFC wrote the paper. AB reviewed the paper. All authors have read and approved the final version of the paper.

REFERENCES

Banki K, Hutter H, Colombo E, Gonchoroff NJ, Perl A.1996. Glutathione levels and sensitivity to apoptosis are regulated by changes in transaldolase expression. J Biol Chem 27: 32994-33001.

Begic A, Djuric A , Gobeljic B , Stevanovic I, Lukic V, Stanojevic I, Nnkovic M, Saso l, Vojvodic D, Djukic M. 2016. The simple isocratic HPLC—UV method for the simultaneous determination of reduced and oxidized glutathione in animal tissue. Acta Chromatographica 29:1-18 https:// doi.org/10.1556/1326.2017.29.1.5

Bergmeyer HU. 1974. Methods of Enzymatic Analysis. London: Verlag Chemie-Academic Press. ISBN:352725370X, 9783527253708

Bracht A, Silveira SS, Castro-Ghizoni CV, Sá-Nakanishi AB, Oliveira MRN, Bersani-Amado CA, Peralta RM, Comar JF. 2016. Oxidative changes in the blood and serum albumin differentiate rats with monoarthritis and polyarthritis. SpringerPlus 5:36-50. http://dx.doi.org/10.1186/s40064-016-1671-1

Castro-Ghizoni CV, Ames APA, Lameira OA, Bersani-Amado CA, Sá-Nakanishi AB, Bracht L, Natali MRM, Peralta RM, Bracht A, Comar JF. 2017. Anti-inflammatory and antioxidant actions of copaiba oil (*Copaifera reticulata*) are associated with histological modifications in the liver of arthritic rats. J Cell Biochem 118:3409-3423. http://dx.doi.org/10.1002/jcb.25998

Comar JF, Sá-Nakanishi AB, Oliveira AL, Wendt MMN, Bersani-Amado CA, Ishii-Iwamoto EL, Peralta RM, Bracht A. 2013. Oxidative state of the liver of rats with adjuvant-induced arthritis. Free Rad Biol Med 58:144-153. http://dx.doi.org/10.1016/j.freeradbiomed.2012.12.003

Comar JF, Suzuki-Kemmelmeier F, Constantin J, Bracht A. 2010. Hepatic zonation of carbon and nitrogen fluxes derived from glutamine and ammonia transformations. J Biomed Sci 17:1. http://dx.doi.org/10.1186/1423-0127-17-1

Comar JF, Suzuki-Kemmelmeier F, Bracht A. 2003. The action of oxybutinin on haemodynamics and metabolism in the perfused rat liver. Basic Clin Pharmacol Toxicol 93:147-152. http://dx.doi.org/10.1034/j.1600-0773.2003.930307.x

Dinkova-Kostova AT, Abramov AY. The emerging role of Nrf2 in mitochondrial function, Free Rad. Biol. Med. 88 (2015) 179-188. http//doi.org/10.1016/j.freeradbiomed.2015.04.036

Eggleston LV, Krebs HA. 1974. Regulation of the pentose phosphate cycle. Biochem J 138: 425-435. PMCID: PMC1166228

Fahim AT, Abd-el Fattah AA, Agha AM, Gad MZ. 1995. Effect of pumpkin-seed on the level of free radical scavenger induced during adjuvant arthritis in rats. Pharmacol Res 31:73-79. https://doi.org/10.1016/1043-6618(95)80051-4

Fedatto Z Jr, Ishii-Iwamoto EL, Caparroz-Assef SM, B, Vicentini G, Bracht A. Kelmer-Bracht AM. 2002. Glycogen levels and glycogen catabolism in livers from arthritic rats. Mol Cell Biochem 229: 1-7. https://doi.org/ 10.1023/A:1017913124084

Fedatto Z Jr, Ishii-Iwamoto EL, Amado CB, Maciel ERM, Bracht A, Kelmer-Bracht AM.2000. Glucose phosphorylation capacity and glycolysis in the liver of arthritic rats. Inflamm Res 49: 128-132. https://doi.org/10.1007/s000110050570

Fedatto Z Jr, Ishii-Iwamoto EL, Amado CB, Vicentini G, D'urso-Panerari A, Bracht A. Kelmer-Bracht AM. 1999. Gluconeogenesis in the liver of arthritic rats. Cell Biochem Funct, 17: 271-278.
doi.org/10.1002/(SICI)1099-0844(199912)17:4<271::AID-CBF839>3.0.CO;2-P

Guo Y, Yu S, Zhang C, Kong ANT. Epigenetic regulation of keap1-Nrf2 signaling. Free Rad. Biol. Med. 88 (2015) 337-349.
http//doi.org/10.1016/j.freeradbiomed.2015.06.013

Hegen M, Keith Jr JC, Collins M, Nickerson-Nutter CL.2008. Utility of animal models for identification potential therapeutics for rheumatoid arthritis. Ann Rheum Dis 67:1505-1515. http://dx.doi.org/10.1136/ard.2007.076430

Heinrich PC, Morris HP, Weber G. 1976. Behavior of transaldolase (EC 2.2.1.2) and transketolase (EC 2.2.1.1) activities in normal, neoplastic, differentiating, and regenerating liver. Cancer Res 36:3189-3197.

Kalhorn TF, Thummel KE, Nelson SD, Slattery JT. 1985. Analysis of Oxidized and Reduced Pyridine Dinucleotides in Rat Liver by High-Performance Liquid Chromatography. Analytical Biochemistry 151: 343-347.
https://doi.org/10.1016/0003-2697(85)90185-X

Katz J, Wood HG. 1963. The use of $^{14}CO_2$ yields from glucose-1- and 6-C^{14} for the evaluation of the pathways of glucose metabolism. J Biol Chem. 238:517-523.

Kim J, Cha Y-N, Surh Y-J. 2010. A protective role of nuclear factor-erythroid 2-related factor-2 (Nrf2) in inflammatory disorders. Mutation Res 690:12–23.
https://doi.org/10.1016/j.mrfmmm.2009.09.007

Kitas GD, Gabriel SE. 2011. Cardiovascular disease in rheumatoid arthritis: state of the art and future perspectives. Ann Rheum Dis 70:8-14.

Larrabee MG. 1990. Evaluation of the pentose phosphate pathway from 14CO2 data. Fallibility of a classic equation when applied to non-homogeneous tissues. Biochemical J 272:127-132. https://doi.org/10.1042/bj2720127

Lemarechal H, Allanore Y, Chenevier-Gobeaux C, Kahan A, Ekindjian OG, Borderie D. 2006. Serum protein oxidation in patients with rheumatoid arthritis and effects of infliximab therapy. Clin Chimica Acta 372:147-153. https://doi.org/10.1016/j.cca.2006.04.002

McInnes IB, Schett G. 2011. The pathogenesis of rheumatoid arthritis. N. Engl. J. Med. 365:2205–2219. https://doi.org/10.1056/NEJMra1004965

Misko TP, Radabaugh MR, Highkin M, Abrams M, Friese O, Gallavan R, Bramson C, Hellio le Graverand MP, Lohmander LS, Roman D. 2013. Characterization of nitrotyrosine as a biomarker for arthritis and joint injury. Osteoarthritis Cart 21:151-156. https://doi.org/10.1016/j.joca.2012.09.005

Novello F, Mclean P. 1968. The pentose phosphate pathway of glucose metabolism. Measurement of the non-oxidative reactions of the cycle. Biochem J 107:775-791.

Roubenoff, R. 2009. Rheumatoid cachexia: a complication of rheumatoid arthritis moves into the 21st century. Arthritis Res Ther 11:108-109. http://doi.org/10.1186/ar2658

Sá-Nakanishi AB, Neto JS, Moreira LS, Gonçalves GA, Silva FMS; Bracht L, Bersani-Amado CA, Peralta RM; Bracht A, Comar JF. 2018. Anti-inflammatory and antioxidant actions of methyl jasmonate are associated with metabolic modifications in the liver of arthritic rats. Biochimie, submitted.

Schubert AC, Wendt MMN, Sá-Nakanishi AB, Bersani-Amado CA, Peralta RM, Comar JF, Bracht A. 2016. Oxidative status and oxidative metabolism of the heart from rats with adjuvant-induced arthritis. Exp Mol Pathol, 100:393-401. http://dx.doi.org/10.1016/j.yexmp.2016.03.005

Sonkoly E, Pivarcsi A. Advances in microRNAs: implications for immunity and inflammatory diseases, J. Cell. Mol. Med. 13 (2009) 24-38. http://doi.org/10.1111/j.1582-4934.2008.00534.x

Stincone A, Prigione A, Cramer T, Wamelink MMC, Campbell K, Cheung E, Olin-Sandoval V, Grüning NM, Krüger A, Alam MT, Keller MA, Breitenbach M, Brindle KM, Rabinowitz JD, Ralser M. 2015. The return of metabolism: biochemistry and physiology of the pentose phosphate pathway. Biol Rev 90:927–963. http://dx.doi.org/10.1111/brv.12140

Stolina M, Bolon B, Middleton S, Dwyer D, Brown H, Duryea D. 2009. The evolving systemic and local biomarker milieu at different stages of disease progression in rat adjuvant-induced arthritis. J Clin Immunol 29:158-174. http://doi.org/ 10.1007/s10875-008-9238-8.

Summers GD, Metsios GS, Stavropoulos-Kalinoglou A, Kitas GD.2010. Rheumatoid cachexia and cardiovascular disease. Nat Rev Rheumatol 6:445–451. http://doi:10.1038/nrrheum.2010.105

Stamp LK, Khalilova I, Tarr JM, Senthilmhan R, Turner R, Haigh RC, Winyard PG, Kettle AJ. 2012. Myeloperoxidase and oxidative stress in rheumatoid arthritis. Rheumatology 51:1796-1803. https://doi.org/10.1093/rheumatology/kes193

Uhlig T, Moe RH, Kvien TK. 2014.The burden of disease in rheumatoid arthritis. Pharmacoeconomics 32:841-851. http://doi.org/10.1007/s40273-014-0174-6

Von Haehling S, Anker SD. 2014. Prevalence, incidence and clinical impact of cachexia: facts and numbers—update J Cachexia Sarcopenia Muscle. 2014 5(4): 261–263. http://doi.org/10.1007/s13539-014-0164-8

Yasmineh WG, Parkin JL, Caspers JI, Theologides A. 1991. Tumor necrosis factor/cachectin decreases catalase activity of rat liver. Cancer Res 51:3990-3995. http://doi.org/10.1172/JCI116225

Yasmineh WG, Theologides A. 1992. Effect of tumor necrosis factor on enzymes of gluconeogenesis in the rat. Proceedings of the Society for Experimental Biology and Medicine 199:97-103.
http://doi/abs/10.3181/00379727-199-43336

Wendt MMN, Sá-Nakanishi AB, Ghizoni CVC, Bersani-Amado CA, Peralta RM, Bracht A, COMAR JF. 2015. Oxidative state and oxidative metabolism in the brain of rats with adjuvant-induced arthritis. Exp Mol Pathol 98:549-557. http://dx.doi.org/10.1016/j.yexmp.2015.04.002

Wendt MMN, Franco-Salla GB, Santos LC, Parizotto AV, Bersani-Amado CA, Bracht A, Comar FC. 2018. Fatty acids uptake and oxidation are increased in the liver of rats with adjuvant-induced arthritis. Journal of Cellular Biochemistry, submitted.

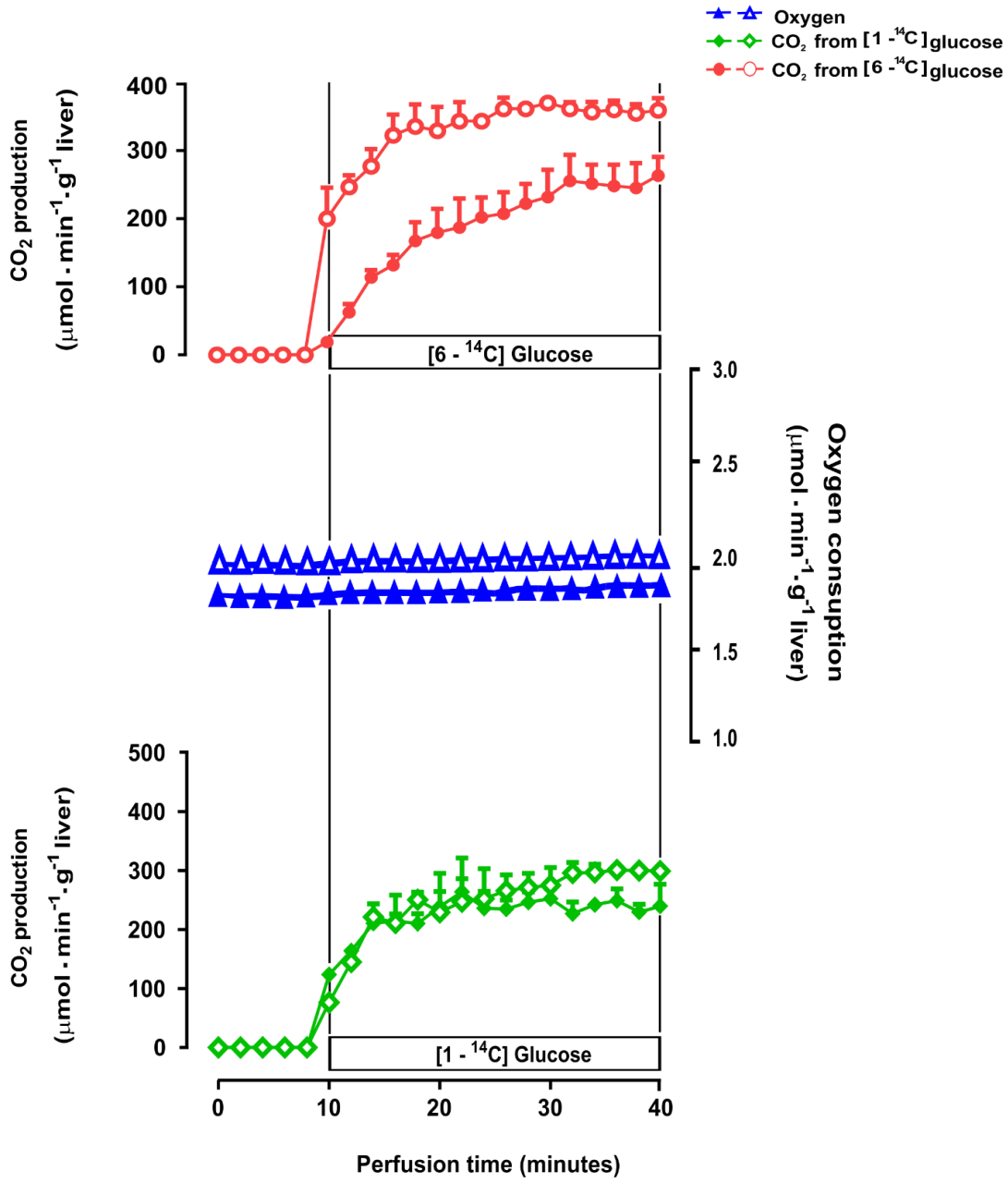

Figure 1. **Time courses of CO2 production and oxygen consumption in the fed rat livers perfused with 10 mM glucose.** Livers from fed controls and arthritic rats were perfused with Krebs/Henseleit-bicarbonate buffer. Glucose (10 mM) plus traces amount of [1-^{14}C]glucose or [6-^{14}C]glucose (0.2 µCi·mL^{-1}) were infused during 30 minutes (horizontal bars). $^{14}CO_2$ production was measured by spectroscopy of liquid scintillation and oxygen uptake was monitored by polarography. Data are the mean ± SEM from four liver perfusion experiments for each condition. Full symbols (● ♦ ▲) represent control rats and empty symbols (○ ◇ △) represent arthritis rats.

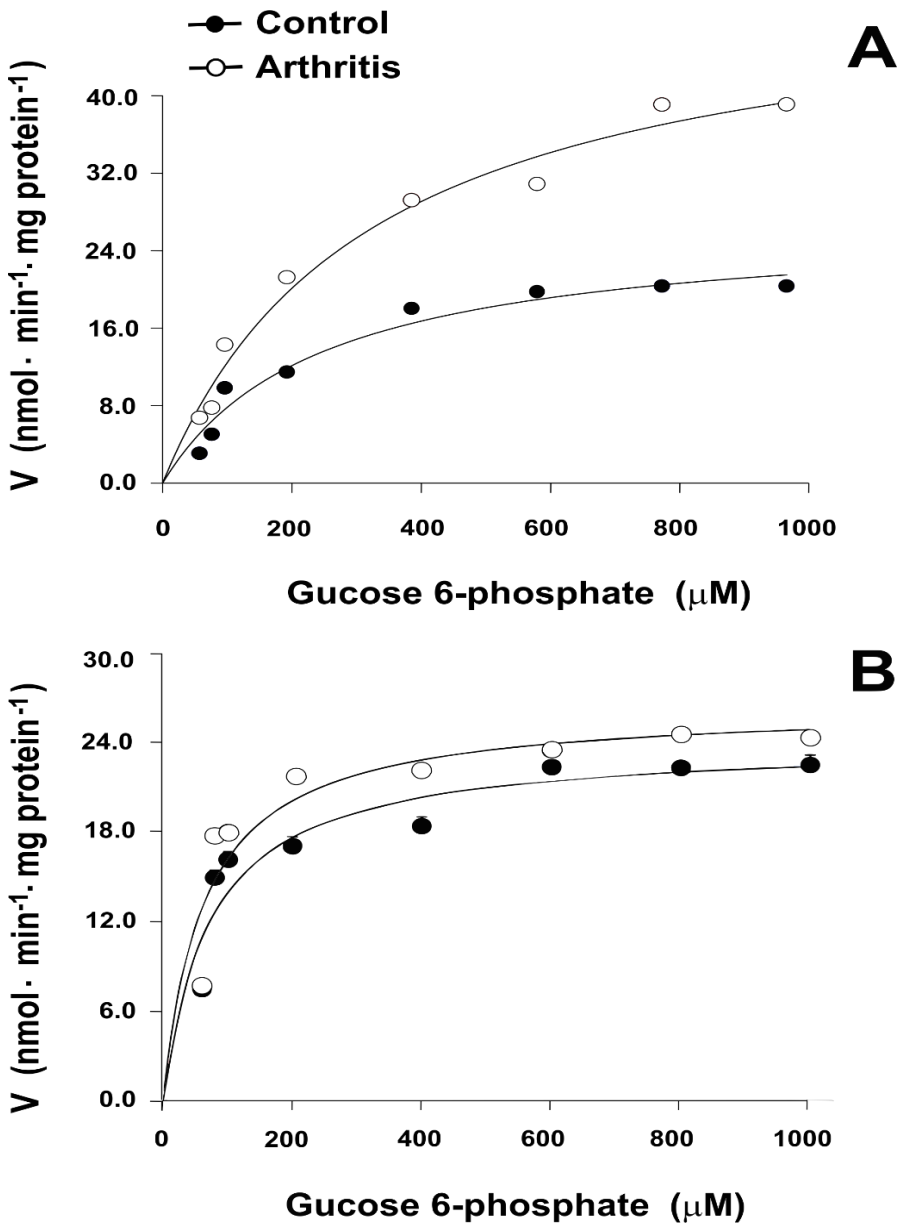

Figure 2. Activity of hepatic glucose 6-phosphate dehydrogenase (G6PDH) from control and arthritic rats in the fasted (A) and fed (B) states as a function of glucose 6-phosphate concentration. The experimental points are means±SEM of 6 animals in each experimental condition. The continuous lines were calculated by means of the Michaelis-Menten equation with optimized values for K_M and V_{max}. These parameters were optimized by means of a nonlinear least-squares procedure. Their values are: (A) fasted control: K_M = 243.8±56.4 μM and V_{max} = 26.9±2.2 nmol·min^{-1}·mg^{-1}, fasted arthritic K_M =320.3±57. 7 μM and V_{max} = 52.44±3.7 nmol·min^{-1}·mg^{-1}, (B) fed control: K_M = 69.5±18.1 μM and V_{max} = 23.8±1.5 nmol·min^{-1}·mg^{-1}, fed arthritis K_M = 60.9±18.4 μM and V_{max} = 26.2±1.78 nmol·min^{-1}·mg^{-1}.

Table I. ***Metabolic rates in the pentose phosphate pathway and the levels of adenine dinucleotides and glycogen in the perfused livers.*** The livers of fed rats were perfused with 10 mM glucose plus traces amount of [1-^{14}C]glucose or [6-^{14}C]glucose (0.2 μCi·mL^{-1}). The values of CO_2 are the rate of each parameter at 40 minutes perfusion time in Figure 1 (steady-state). ΔOxygen consumption is the increment of this parameter due to 10 mM glucose infusion. Glucose uptake (G) was calculated as glucose infusion rate before entering the liver less that rate in the effluent perfusate. The fraction of glucose metabolized in PPP (Fmet) was calculated as equation (1) described in Methods. Hepatic content of glycogen and adenine dinucleotides were measured in the perfused liver freeze-clamped in the end of the glucose infusion (40 min perfusion time in Figure 1).

Parameters	Control	Arthritis

CO_2 production from [1-^{14}C]glucose (μmol·min^{-1}·g^{-1})	0.241 ± 0.011	0.300 ± 0.011$^{\#}$
CO_2 production from [6-^{14}C]glucose (μmol·min^{-1}·g^{-1})	0.263 ± 0.018	0.358 ± 0.014*
ΔOxygen consumption (μmol·min^{-1}·g^{-1})	0.064 ± 0.02	0.068 ± 0.01

Parameters	Fasted		Fed	
	Control	Arthritis	Control	Arthritis
GSH (nmol·g^{-1} liver)	34.8 ± 1.8	28.3 ± 0.1$^{\#}$	50.0 ± 3.2	32.1 ± 1.9$^{\#}$
GSSG (nmol·g^{-1} liver)	1.59 ± 0.26	2.36 ± 0.02$^{\#}$	1.52 ± 0.04	1.42 ± 0.07
GSH+2xGSSG (nmol·g^{-1} liver)	38.6 ± 1.6	31.1 ± 0.8*	52.0 ± 4.4	33.7 ± 2.1$^{\#\#}$
GSH/GSSG	22.0 ± 1.0	12.0 ± 0.1$^{\#}$	33.0 ± 2.0	23.1 ± 0.7$^{*\#}$
Glucose-6-phosphate (nmol·g^{-1} liver)	1.7 ± 0.02	2.1 ± 0.1*	1.8 ± 0.1	2.4 ± 0.1**
Glycogen (μmol glycosil units.gram liver^{-1})	408.3 ± 38.4		100.2 ± 4.3**	
Adenine Nucleotides				
NADP^{+} (μmol·g fresh liver^{-1})	0.113 ± 0.008		0.106 ± 0.005	
NADPH (μmol·g fresh liver^{-1})	0.314 ± 0.017		0.152 ± 0.015	
Enzymatic activity				
NADPH/NADP^{+}	2.418 ± 0.150		1.642 ±0.131*	
NADH/NAD^{+}	0.131 ± 0.008		0.106 ± 0.005$^{\#}$	

Data are the mean ± SEM of 4-6 animals in each experimental condition. Pairs of values in the same line with superscripts are different: $^{\#}$p<0.05, *p<0.01, **p<0.001.

G6PDH ($nmol \cdot min^{-1} \cdot mg^{-1}$)	20.3 ± 0.5	39.1 ± 0.6**	22.3 ± 0.7	24.1 ± 0.1$^{\#}$
Transaldolase ($nmol \cdot min^{-1} \cdot mg^{-1}$)	3.4 ± 0.1	5.3 ± 0.3*	14.8 ±0.8	14.2 ± 0.9

Table II. **Hepatic levels of glutathione, glucose-6-phosphate and activity of glucose 6-phosphate dehydrogenase (G6PDH) and transaldolase**. The parameters were determined in liver from fasted and fed control and arthritic rats as described in Methods.

Data are the mean ± SEM of six animals in each experimental condition. Pairs of values in the same line labelled with superscripts are different: $^{\#}p<0.05$, $^{*}p<0.01$, $^{**}p<0.001$.